Comparative analysis of DREB gene family in buckwheat: the role of FtDREB02 in the delphinidin biosynthesis and drought stress response

Jing Wang[1,2,3,5†], Yanhua Chen[1,5†], Fan Dongqing[1,5†], Yuqi He[1,5], Chaonan Guan[1], Yaliang Shi[1], Xiangru Wang[1], Hao Lin[1], Marie-Laure Fauconnier[2], Giorgia Purcaro[3], Muriel Quinet[4], Manon Genva[2], Rintu Jha[1], Kaixuan Zhang[1,5], and Meiliang Zhou[1,5*]

[1]National Key Facility for Crop Gene Resources and Genetic Improvement Institute of Crop Sciences, Chinese Academy of Agricultural Sciences, Beijing 100081, China.

[2]The Laboratory of Chemistry of Natural Molecules, Gembloux Agro-Bio Tech, University of Liè ge, Passage des Déportés, 2 - 5030 Gembloux, Belgium.

[3]The Analytical Chemistry Lab, Chemistry for Sustainable Food and Environmental Systems, Gembloux Agro-Bio Tech, University of Liège, Bât. G1,Passage des Déportés 2, 5030 Gembloux, Belgium.

[4]Groupe de Recherche en Physiologie Végétale (GRPV) Earth and Life Institute-Agronomy (ELI-A) Université Catholique de Louvain Croix du Sud 45, boîte L7.07.13, Louvain-la-Neuve B-1348, Belgium.

[5]Sanya Nan Fan Research Institute, Chinese Academy of Agricultural Sciences, Sanya, 572024, Hainan, China.

† Equal contributors

***Corresponding author:**

Meiliang Zhou

National Key Facility for Crop Gene Resources and Genetic Improvement Institute of Crop Sciences, Chinese Academy of Agricultural Sciences, Beijing 100081, China.

Sanya Nan Fan Research Institute, Chinese Academy of Agricultural Sciences, Sanya, 572024, Hainan, China.

Tel.: 010-82106368; Email: zhoumeiliang@caas.cn.

SUMMARY

Dehydration response element binding (DREB) transcription factors play a pivotal role in plant abiotic stress responses, but its evolutionary and functional characterization in buckwheat remains unexplored. Here, we conducted a comprehensive analysis of the *DREB* gene family across three buckwheat species, revealing segmental duplication as the primary driver of family expansion and potential purifying selection during evolution. A *FtDREB02* gene, classified as group A2, was identified through Genome-wide association analysis (GWAS) on drought tolerance and delphinidin content. Functional validation in *Arabidopsis thaliana* and hairy root of Tartary buckwheat (*Fagopyrum tataricum*) demonstrated that overexpression of this gene promotes delphinidin biosynthesis and enhances plant resistance to water scarcity. Through the integration of DAP-seq and PEG transcriptome cluster analysis, A *FtANS* candidate was screened. Functional studies showed that *FtDREB02* regulates delphinidin content by binding directly to DRE elements of *FtANS* promoter. This research identifies and comprehensively analyzes the DREB family within buckwheat species, elucidating the regulatory mechanisms of *FtDREB02* in controlling flavonoid biosynthesis and drought resistance, providing potential genetic resources for breeding buckwheat varieties with excellent agronomic traits.

Keywords: buckwheat, DREB family, delphinidin, drought stress

INTRODUCTION

The intensification of extreme climate, driven by global warming, poses a significant challenge to agricultural production at present and in the future (Wang et al., 2023; Seth and Sebastian, 2024). Drought stress is a critical factor impacting crop yield and quality, with significant threats to the sustainable development goal of achieving 'zero hunger' by 2030 (Otekunrin, 2021; Yin and Slater, 2023; Tarolli and Zhao, 2023; Wei et al., 2024). As sessile organisms, plants primarily respond to stress through escape, avoidance or tolerance mechanisms (Kershaw and Levitt, 1973; Barton and Koricheva, 2010; Rauschkolb et al., 2022), such as early flowering (Metz et al., 2020), the formation of longer roots (Cella Pizarro and Bisigato, 2010) or altered osmotic potential (Májeková et al., 2019). Therefore, it is essential to utilize excellent germplasm to obtain potential gene resources and improve the adaptability of crops to adversity through modern biotechnology to feed the growing global population (Bailey-Serres et al., 2019; Sun et al., 2022).

Buckwheat belongs to the *Fagopyrum* genus within the Polygonaceae family, serving as underutilized grain crop. Tartary buckwheat (*Fagopyrum tataricum*) and common buckwheat (*Fagopyrum esculentum*) are the most widely cultivated species, while golden buckwheat (*Fagopyrum dibotrys*) is a wild relative of these cultivated varieties (He et al., 2022). Tartary buckwheat and common buckwheat, obtained through two independent domestication events, are widely cultivated as functional food crops due to their abundant bioactive compounds and exceptional nutritional value (Wijngaard and Arendt, 2006; Jing et al., 2016; Jha et al., 2024). The wild relative golden buckwheat, particularly valued for the pharmacological properties of its tuberous rhizomes (as the traditional medicinal organ, distinct from true roots morphologically and functionally), has been extensively utilized in traditional Chinese medicine (He et al., 2022). Moreover, buckwheat has the advantages of a short growing season and strong adaptability to environmental conditions. It is widely cultivated in mountainous, arid and semi-arid regions, demonstrating excellent drought tolerance (Wen et al., 2021; He et al., 2024). Numerous studies have demonstrated that plants under drought stress produce increased levels of secondary metabolites, especially flavonoids. For instance, under water stress, the content of anthocyanins, delphinidin and their derivatives in roselle changed significantly (Hinojosa-Gómez et al., 2020). These substances could help mitigate the accumulation of reactive oxygen species (ROS) during prolonged drought conditions (Nakabayashi et al., 2014; Tiedge et al., 2022; La et al., 2023). Although buckwheat has also shown changes in phenolic compounds during drought stress (Wang et al., 2023; Oksana et al., 2023), it is quite unclear how these changes occur molecularly.

Transcription factors (TFs), also known as trans-acting factors, are a class of key proteins that are notably involved in network regulation in plant response to environmrnt stress, acting as molecular regulatory switches (Gahlaut et al., 2016; Khan et al., 2018). Dehydration response element binding (DREB) proteins are a large class of transcription factors belonging to the AP2/ERF subfamily members, which includes a typical AP2 domain roughly 60 amino acids. The valine (Val) at position 14 and the glutamic acid (Glu) at position 19 are essential residues for this family to identify and bind to DNA elements (Riechmann and Meyerowitz, 1998; Lata and Prasad, 2011; Agarwal et al., 2017). It is well known that *DREBs* participate in drought response in many crops, such as rice (Dubouzet et al., 2003; Wang et al., 2008), wheat (Mei et al., 2022), barley (Morran et al., 2011), soybean (Zhou et al., 2020), sugarcane (Reis et al., 2014), cowpea (Kumar et al., 2022), banana (Xu et al., 2023), bamboo (Hu et al., 2023), etc. Furthermore, *DREBs* have additionally been implicated in regulating the biosynthesis of plant phenols, phenanthroquinones, and flavonoids,

which is induced by the drought stress. Specifically, overexpression of the *AtDREB1A* gene leads to an enhanced drought resistance in *Arabidopsis* and increased content of salvianolic acids and tanshinones in *Salvia miltiorrhiza* roots (Wei et al., 2016). Similarly, *AmDREB3* from *Ammopiptanthus mongolicus* affects anthocyanin synthesis in *Arabidopsis* seedlings under drought stress (Ren et al., 2019). Additionally, *CitERF32* and *CitERF33* promote flavonoid accumulation by binding to the promoter of the *CitCHIL1* gene in citrus (Zhao et al., 2021). Thus, *DREB* genes offer a promising option for developing nutrient-rich and resilient to water scarcity crops (Sarkar et al., 2019).

In this study, the *DREB* gene family were identified in three buckwheat species, and their gene structures and evolutionary relationships were analyzed. Combined with metabolites and drought phenotype data, GWAS identified a candidate *FtDREB02* gene that may be associated with delphinidin biosynthesis and drought response. The potential biological functions of transgenic lines in Tartary buckwheat hair root and *Arabidopsis* were elucidated by characterizing the metabolite composition, physiological index differences and plant phenotypic alterations. Its downstream target gene, *FtANS*, was identified by a combination of DAP-seq and PEG transcriptome cluster analysis, and its molecular regulatory mechanism was analyzed by protein-promoter interaction experiment. This study enhances our understanding of the evolutionary patterns and functional characteristics of the *DREB* gene family in different buckwheat species, clarifies the gene function and molecular mechanism of *FtDREB02*, and offers valuable gene resources for future smart crop breeding.

RESULTS

Identification and characterization of *DREB* gene family in buckwheat

Herein, we systematically characterized DREB genes across three representative buckwheat species - *F. dibotrys* (the wild relative), *F. esculentum* and *F. tataricum* (main cultivated species), and finally identified 36 *FdDREBs*, 52 *FeDREBs,* and 46 *FtDREBs* containing the AP2 domain (PF00847) by BLASTP search and Hidden Markov Model search (HMM) (Table S1) (He et al., 2022). These DREB proteins were further named according to their location on chromosomes. The range of molecular weight and theoretical isoelectric point (PI) of DREB proteins in three buckwheat species were found to be relatively close, with *F. dibotrys* being the narrowest, ranging from 119 amino acids to 328 (13.05KD-36.15KD), and PI from 4.6 to 9.49. The distribution range of physicochemical properties in *F. tataricum* was relatively wider, spanning from 116 to 377 amino acids (12.59KD-41.63KD), with PI ranging from 4.32 to 10.56. The widest range was highlighted for *F. esculentum* from 115 to 452 (12.48-49.4KD), with PI from 4.63 to 11.6 (Table S1). Multiple sequence alignment revealed that the DREB family in buckwheat has two fragments of conserved domains: the N-terminal hydrophilic YRG element (considered to be involved in DNA-binding) and the RAYD element with amphipathic α-helical characteristics (considered to be involved in protein-protein interaction) (Figure 1a-c, S1). Its three-dimensional structure contains three antiparallel β-sheets and one α-helix (Figure 1c, S2). All DREB proteins have valine (V) at position 13/14, and the amino acid at position 18/19 is mainly glutamic acid (E) (Figure 1c, S1), a well-known feature of the DREB family.

We used information from all of the *DREBs* found in the three buckwheat species to generate a thorough phylogenetic tree that included 56 AtDREBs from *A.thaliana* in order to clarify the taxonomy and evolutionary dynamics of *DREB* genes. The analysis revealed that the combined dataset of the 190 genes could be grouped into six distinct groups designated from A1 to A6 (Figure 1d). Notably, the distribution of *DREB* genes among *F. dibotrys*, *F. esculentum*, and *F. tataricum*

were found to be similar. For example, the largest number was found in group A4, followed by A6, and the least in group A1. This pattern could be correlate with the evolutionary relationship between the three buckwheat species.

Chromosome location, collinearity, duplication, and expansion of *DREB* genes

A comprehensive gene mapping analysis was conducted to determine the chromosomal localization of *DREB* genes in buckwheat. The results showed that the *DREB* genes exhibited an uneven distribution across the eight chromosomes in three buckwheat species *F. dibotrys* (Figure S3a) and *F. tataricum* (Figure S3c) possess the highest number of *DREB* genes on their chromosome 8, while *F. esculentum* had the highest number of *DREB* genes on chromosome 3 (Figure S3b). In the process of biological evolution, gene expansion, and contraction are two important strategies for plants to adapt to the environment and form species diversity. Gene duplication events play an indispensable role in this process (Panchy et al., 2016). Utilizing the MCScanX method, we analyzed the gene duplication events within the DREB family in buckwheat. The results showed that only one pair of tandem repeats existed in *F. tataricum* across three buckwheat species (Table S2). There were a large number of segmental duplication events in three buckwheat species, including 10, 14, and 16 pairs respectively in *F. dibotrys*, *F. esculentum*, and *F. tataricum* (Figure S4, Table S2). As previously documented, *F. dibotrys* is a perennial wild relative predominantly distributed in southwestern China and Southeast Asia, whereas *F. esculentum* and *F. tataricum* are annual cultivated species with a broad geographical range, including Asia, Europe, and the Americas (Zhang et al., 2021; He et al., 2022; Zhang et al., 2023). This implies that segmental duplication events are the main driver for the expansion of the *DREB* gene family in buckwheat, and the frequency of duplication may be associated with ecological divergence among species.

To understand the evolutionary history of the DREB family, we further analyzed the collinearity among three buckwheat species. 30 *FdDREBs* showed collinearity relationships with *F. esculentum*, and 31 pairs of orthologous genes between *F. dibotrys* and *F. tataricum* (Figure 2a, Table S2). It is worth noting that, among the homologous genes between *F. dibotrys* and *F. esculentum*, except for *FD05G039190.1*, the remaining 29 were present in *F. dibotrys* and *F. tataricum* (Figure S5, Table S2). This findings showed that although these 29 genes underwent multiple duplication events during the evolutionary transitions from *F. dibotrys* to *F. esculentum* and *F. tataricum*, they were not lost or changed, suggesting that these genes may play crucial functional roles in buckwheat species.

In order to gain insight into the evolutionary process and selection pressure acting on DREB family, we calculated the Ka/Ks ratios within and between buckwheat species. The results showed that all duplication events within species exhibited negative selection, as evidenced by Ka/Ks values ranging from 0.1197 to 0.8501 (Table S2). Among the inter-species duplication events, only the gene pair *FdDREB36* and *FtDREB46* showed positive selection, with a Ka/Ks ratio of 1.095. The remaining gene pairs exhibited Ka/Ks values below 1, indicating purifying selection. The effective Ka/Ks values of *F. dibotrys* and *F. esculentum* ranged from 0.0822 to 0.8442, and those for *F. dibotrys* - *F. tataricum* pair were within a broader range 0.0297-1.0951 (Table S2). These findings suggest that the DREB family may have experienced purifying selection during buckwheat evolution.

Gene structure, motif, and cis-regulatory elements analysis of *DREBs*

To understand the structural characteristics of the DREB family in buckwheat, we analyzed the sequence structure and conserved motifs of the genes and predicted a total of 10 motifs, which were

named in the order of 1-10 (Table S3). Family members within the same group exhibited similar motif compositions and arrangement orders (Figure S6, Table S3). For example, the A4 group in *F. tataricum* is primarily composed of motif 2, motif 1, motif 3 (Figure S6c), and the A5 group in *F. esculentum* is mainly composed of motif 3, motif 1, motif 2 (Figure S6b).

Cis-regulatory elements (CREs) are specific DNA sequences located in the promoter region of genes that can be bound by TFs, thereby influencing plant growth, development, or responses to environmental stresses. To further understand the function of the DREB family in plants, we predicted the CREs (cis-regulatory elements) in the 2kb sequence upstream of the transcription start site (TSS) of each gene on the Plantcare website. These CREs can be categorized into three main types. The first one is growth and development elements, such as circadian rhythm-related elements, meristem-specific elements, endosperm expression elements, seed-specific regulatory elements, etc. Second one is stress response elements, like defense response elements, drought-related elements, wound response elements, etc. The last one is hormone response elements, including jasmonic acid response elements, abscisic acid response elements, auxin response elements, gibberellin response elements, etc. Light response elements were the most abundant across the three species, followed by jasmonic acid response elements. Among the environmental stress-related elements, low-temperature and drought response elements showed higher content, while less wound response elements were involved (Table S4). Interestingly, the number of these CREs was found to be higher in *FeDREBs* and *FtDREBs* than in *FdDREBs* (Figure S6, Table S4). This suggests that gene functions within the DREB family are conserved among different buckwheat species, and that evolutionary variation in the number of CREs likely be associated with differences in growth, development, and environmental adaptability between cultivated and wild populations.

Expression pattern of *DREBs* in buckwheat

The relative expression of genes in different tissues and under stress treatment is closely related to their biological functions. Consequently, we analyzed the relative expression of *DREBs* in different tissue of three buckwheat species (Hou et al., 2021; He et al., 2022; Lin et al., 2023). Expression heatmap analysis revealed tissue-specific patterns of DREB family across three buckwheat species (Figure 2b-c, S7), which showed that 39% of *DREB* genes (14/36) showed highest expression in rhizome of golden buckwheat, with analogous trends observed in root of common buckwheat (29%, 15/52) and Tartary buckwheat (43%, 20/46) (Table S5). Remarkably, the roots of the cultivated buckwheat have a very high flavonoid content, while the rhizome of *F. dibotrys* retains a highly appreciated diverse medicinal ingredients (He et al., 2022; Zhang et al., 2023). Simultaneously, the root represents the first organ to sense water stress in plants, suggesting a possible link between the metabolites and drought response in Tartary buckwheat (Yang et al., 2022; Wang et al., 2024).

To better understand how *DREBs* respond to drought stress, we utilized 20% PEG 6000 transcriptome in *F. tataricum*, retrieved from the China National Center for Bioinformation Genome Sequence Archive (accession number: PRJCA003569), to construct a heat map of *FtDREBs* expression (Huang et al., 2021). The map revealed that most members of the A2/A3 group were induced under drought conditions (Figure 2c). Furthermore, the A6 group members showed distinct increases of relative expression after PEG treatment (Figure 2c).

Mining and identification of drought-responsive genes associated with flavonoids by GWAS

There exists an inextricable relationship between plant secondary metabolites and environmental stress responses (Jogawat et al., 2021; Changan et al., 2023). *F. tataricum* is

particularly abundant in flavonoids, such as kaempferol, quercetin, rutin, which are not only possess pharmacological properties but may also influence drought stress responses (Wang et al., 2023; Oksana et al., 2023; Luo et al., 2024; He et al., 2024; Gao et al., 2025). To investigate potential genetic interactions, parallel GWAS analyses were performed using characterized drought-responsive phenotypic data, delphinidin content metrics, and resequencing datasets, which collectively identified *FtDREB02* as a unique DREB locus exhibiting the most immediate and pronounced upregulation (nearly 2.5-fold induction within 1 h) in 20% PEG-6000 transcriptomes (Figure 3a, S8-9; Table S6-7) (Zhao et al., 2023; He et al., 2024; Lai et al., 2024).

Our sequence analysis revealed that SNP variants in Tartary buckwheat were exclusively located within 800 bp upstream of the ATG start codon in the promoter region, with no variants detected in exons or untranslated regions (UTRs) (Figure 3b). To investigate potential functional consequences of these promoter SNPs, we performed cis-regulatory element (CRE) prediction using PlantPAN 4.0 on variation sites, which identified potential binding sites for several transcription factors that may be affected by the SNPs, including LBD (SNP-790), ERF (SNP-287), MYB (SNP-287), C2H2 (SNP-107), and bZIP (SNP-107) etc (Table S8), suggesting these SNPs may potentially influence the regulatory control of *FtDREB02* by these TFs. Comparative sequence analysis of the target gene across three buckwheat species revealed limited intraspecific variation but substantial interspecific divergence, particularly in common buckwheat (Figure 3c, S10). Relative to Tartary buckwheat and golden buckwheat, common buckwheat exhibited significantly higher polymorphism, including multiple non-synonymous SNPs and a critical 27-bp indel within the N-terminal conserved domain (Figure 3c). Subsequent quantification of delphinidin content across these species demonstrated markedly lower accumulation in common buckwheat compared to Tartary buckwheat and golden buckwheat (Figure 3d, Table S9). This further suggests a potential association between *FtDREB02* and delphinidin content.

Under osmotic stress induced by 20% PEG-6000 treatment, *FtDREB02* transcript levels in Tartary buckwheat exhibited rapid and significant induction, reaching near 5-fold upregulation within 1 hour of stress exposure, which is consistent with transcriptome (Figure 3e, Table S10). The Weighted Gene Co-Expression Network Analysis (WGCNA) of PEG transcriptome revealed that in the blue3 module containing *FtDREB02*, there were many genes related to delphinidin synthesis, including chalcone isomerase (CHS), flavones 3-hydroxylase (F3H), and anthocyanidin synthase (ANS) (Table S23). Among the top 50 genes identified in this network, we observed drought-related regulators such as PDCB3, NAC, MYB, etc (Figure 3f, Table S11). This suggesting that this gene may affect the response to drought conditions and delphinidin metabolism in Tartary buckwheat. Therefore, we selected *FtDREB02* to explore further the molecular mechanism underlying the interaction between flavonoids and drought stress in *F. tataricum*.

Overexpression of *FtDREB02* contributes to delphinidin biosynthesis and drought resistance in *Arabidopsis* and *F. tataricum*.

In order to explore the effect of *FtDREB02* in flavonoid metabolism, we first constructed hairy roots of overexpressing *FtDREB02* in *F. tataricum*. After 15 days of growth in the MS medium, the changes in flavonoids were detected by Liquid Chromatograph-Mass Spectrometer (LC-MS). It was found that delphinidin content increased significantly after *FtDREB02* overexpression (Figure 4a, Table S12), while cyanidin concentration also showed a significant increase. The content in dihydrokaempferol, that is the dividing point of the two branches of flavonoids and anthocyanins, increased significantly after overexpression of *FtDREB02*. Kaempferol is the first product of the

flavonol branch, and its content decreased in the overexpression (OE) lines. In addition, there were slight changes in quercetin content and a large drop in rutin, suggesting that the flavonoid synthesis pathway may shift towards anthocyanin accumulation. And following biosynthesis, leucoanthocyanidins and anthocyanidins will progressively transform into catechins, epicatechins, and other proanthocyanidins through reduction, polymerization, and other processes. Our hypothesis was further supported by the results, with these chemicals rising to varied degrees (Figure 4a, Table S12). By adding 20% PEG 6000 treatment to the MS medium to simulate drought stress, after 30 days of culture, we found that, despite the low amount of metabolites accumulated in the hairy roots due to the early growth stage, the delphinidin content in the OE lines was significantly higher than that of *Agrobacterium rhizogenes* A4 control lines. And the substances synthesis of OE lines converged towards the anthocyanin branch (Figure 4a, Table S12). These indicated that *FtDREB02* mediated the synthesis of flavonoids and promoted the anthocyanin accumulation in *F. tataricum*, especially the increase of delphinidin.

To investigate the potential role of *FtDREB02* under drought stress in buckwheat, we observed the physiological changes of hairy roots after 20% PEG 6000 treatment. After culturing in MS containing 20% PEG for 30 days, it was found that OE lines had higher biomass compared to A4 control lines (Figure 4b-c, Table S13). When plants respond to environmental stress, the cell membrane will be subjected to membrane peroxidation, thereby producing malondialdehyde (MDA), and the MDA content can reflect the degree of damage to the plant cell (Wu et al., 2017). We observed that the MDA and antioxidant enzyme contents in hairy roots increased dramatically after 20% PEG 6000 treatment compared with normal culture, with the MDA content of OE lines being lower than that of the control (Figure 4d, Table S13), while the antioxidant enzyme content was higher (Figure 4e-g, Table S13). Furthermore, we observed the opposite results after silencing *FtDREB02* in Tartary buckwheat seeds, namely, a decrease in delphinidin content and an increase in sensitivity to osmotic stress (Figure S11, Table S14). These reciprocal phenotypes collectively support the pivotal role of *FtDREB02* in regulating both secondary metabolism and stress response pathways in buckwheat.

In order to better understand the role of *FtDREB02* in the plant, we constructed *FtDREB2* transgenic *Arabidopsis* and evaluated their tolerance to 150 mM mannitol. There was no significant difference in germination ratio between the OE lines and Col-0 under normal conditions and 150 mM mannitol treatment (Figure S12, Table S15). However, after one week of 150 mM mannitol treatment, the root length of OE lines exceeded that of Col-0 (Figure 5a-b, Table S16). we assessed the drought tolerance of transgenic plants in natural drought condition, and found that higher survival rates in OE lines compared to Col-0 (Figure 5c-d, Table S17). After drought treatment, the MDA content of both Col-0 and OE lines increased, but the MDA content of *FtDREB02* transgenic plants increased less and was significantly lower than that of the control group (Figure 5e, Table S17), indicating that *FtDREB02* overexpression mitigated cell membrane damage in *Arabidopsis*. Moreover, antioxidant enzyme activity was enhanced in OE lines compared to Col-0, with catalase (CAT), Superoxide Dismutase (SOD), and Peroxidase (POD) levels being significantly higher (Figure 5f-h, Table S8), that is, the antioxidant capacity was enhanced. This was further confirmed by DAB and NBT staining (Figure S13). The results demonstrated that *FtDREB02* overexpression enhances the drought resistance in *Arabidopsis*. The above results revealed that overexpression of *FtDREB02* reshaped the synthesis pathway of flavonoid compounds in buckwheat, promoted delphinidin biosynthesis, and enhanced drought tolerance.

Identification of *FtDREB02* target genes by DAP-seq and PEG transcriptome

Through transiently transfecting a FtDREB02-GFP fusion protein into tobacco leaves, we observed that the gene was localized in the nucleus (Figure S14), which implies that it can influence the physiological and biochemical processes in plants by regulating the expression of downstream genes. To identify direct target genes regulated by *FtDREB02*, we initially utilized DAP-seq technology to generate candidate lists. With a p-value threshold of <0.01 as the cutoff, 26,647 putative binding sites were detected (Table S18). The distribution patterns of these peaks in the genetic region were further analyzed, covering the gene bodies, 2kb upstream of TSS to 2kb downstream of the translation termination site (TTS). About 27% of the peaks were located in the gene region, of which 14.75% were in the promoter region, 3.93% in the exon and 3.12% in the intron region (Figure 6a). The 2kb flanking sequences around each peak were analyzed to identify the potential binding motifs of *FtDREB02*. It was found that the motif with TACAT/CCC/AAAAT/GTCA/GC/G (E value = 1x10-34) as the core was highly enriched. In addition, the GCC motif and DRE motif with the core sequence of CGACCCTGCCGCGCC (E value = 1x10-18) and the DRE motif with the core sequence of CTAGTCGCCGACGCT (E value = 1x10-12) were also identified (Figure 6c). KEGG enrichment analysis was further performed to identify biological processes potentially associated with *FtDREB02* binding sites. The results demonstrated significant enrichment in multiple biosynthesis and metabolic pathways, with secondary metabolite biosynthesis showing the highest enrichment (Figure 6b, Table S19). Pathways including amino acid biosynthesis and metabolism, flavonoid biosynthesis, Sugar metabolism and alkaloids biosynthesis were also significantly enriched (Figure 6b). These findings provide additional support for the involvement of *FtDREB02* in the biosynthesis of flavonoid compounds.

FtDREB02 was shown to regulate the delphinidin biosynthesis, which is affected by several key genes (Figure 4a). We hypothesized that *FtDREB02* regulates the flux of metabolites through different branches by activating the expression of specific enzyme genes involved in this pathway, such as flavonol synthase (FLS), dihydroflavonol 4-reductase (DFR), and anthocyanidin synthase (ANS), flavonoid 3', 5'-hydroxylase(F3'5'H), etc, (Sharma et al., 2022; Guo et al., 2023). Therefore, we screened the putative target gene according to the following criteria: binding peaks identified by DAP-seq located in the promoter region; co-clustering with *FtDREB02* in the PEG transcriptome; genes with catalytic associations with key enzymes in the delphinidin biosynthesis pathway (Figure 6d-e, Table S18, S20). Among the selected candidate genes, only one anthocyanin synthase gene, named *FtANS* (ID: *FtPinG0100809600.01.T01*), met the above criteria and was selected for further analysis, which converts leucoanthocyanidins into anthocyanidins, including cyanidin, delphinidin and pelargonium.

***FtDREB02* directly activates *FtANS* expression**

We speculated that *FtDREB02* regulates gene expression by directly binding to the DRE element on the promoter of the target gene. Thus, we analyzed the 2kb sequence upstream of the TSS of *FtANS* and found two DRE elements, of which the element at -713bp upstream of ATG was located near the DAP-seq binding peak (Table S18). This suggests that *FtDREB02* may regulate the *FtANS* expression by binding to the DRE element, which was confirmed by EMSA experiments (Figure 7c). The effect of *FtDREB02* on the *FtANS* promoter was further studied by dual luciferase assay. The results showed that the addition of FtDREB02 protein significantly enhanced the activity of the promoter compared with the empty plasmid (Figure 7a-b, Table S21), indicating that

FtDREB02 can activate the promoter of the *FtANS* gene by binding to the DRE element. In transgenic hairy roots overexpressing *FtDREB02*, qRT-PCR detected that the expression of *FtANS* was significantly upregulated (Figure 7d-e, Table S22). The above results indicates that *FtDREB02* upregulates *FtANS* expression by directly targeting its DRE element on the promoter, thereby interfering with the catalytic synthesis of metabolites, promoting the increase of delphinidin content, and thus improving the drought resistance in *F. tataricum* (Figure 7f).

DISCUSSION

The DREB family has attracted our attention due to its significant role in abiotic stress (Zhu, 2016; Zhang et al., 2022; Mei et al., 2022; Vonapartis et al., 2022; Kidokoro et al., 2023; Zhang et al., 2024). In buckwheat, only the promoter of *FeDREB1* has been identified in *F. esculentum* as being induced by cold and drought stress so far, while no related reports exist for *F. dibotrys* and *F. tataricum* (Fang et al., 2015). In addition, researchers have studied the AP2/ERF family, but their research work was limited to *F. tataricum* (Liu et al., 2019). Therefore, we utilized the genomes of three representative species — *F. dibotrys*, *F. tataricum*, and *F. esculentum* — and identified 36 *FdDREBs*, 52 *FeDREBs* and 46 *FtDREBs* in these species, respectively. The number of *DREB* genes varies in different buckwheat species, and the number of genes in *F. dibotrys* is the least, which may be related to the genetic evolution among the three species. For instance, gene duplication events occurred due to external pressure and self-regulation during the evolution process of the wild species into the cultivated species, increasing the number of genes in cultivated species (Zhang et al., 2021; He et al., 2022). Gene duplication is considered to be a key mechanism driving biological evolution, mainly including transposons, tandem duplications and segmental duplications (Ober, 2005; Flagel and Wendel, 2009; Liang and Schnable, 2018). Among them, segmental duplication is considered to be the main driving force for the expansion of many gene families, which is consistent with the results of the expansion analysis of the DREB family in buckwheat. We observed a higher number of segmental duplications in *F. tataricum* and *F. esculentum* compared to *F. dibotrys*. Considering their phylogenetic relationships and distinct ecological distributions, we speculate that segmental duplications in the DREB family may have played a role in environmental adaptation during buckwheat evolution. Nearly all of the *DREBs* duplicate gene pairs in buckwheat have Ka/Ks values lower than 1, suggesting that the DREB family has experienced significant negative selection during the evolution of buckwheat to eliminate harmful mutations, thereby adapting to changes in the unfavorable external environment (Liu et al., 2008). In the CREs prediction, we discovered that abiotic stress response elements are not limited to a specific grouping, indicating that the functions within the group are not entirely consistent, and there may be functional redundancy or the influence of gene interaction networks (Kizis and Pagès, 2002; Agarwal et al., 2017; Hu et al., 2022). In addition, we found that the difference in numbers between groups is large. This may be related to specific environmental conditions during the evolution of species, such as adapting to adverse external conditions through various gene duplication events to achieve functional superposition or weakening (Magadum et al., 2013). Therefore, the specific functions and contributions of *DREB* genes in each group remain to be further verified.

Tissue specificity and expression profiles of genes after different treatments help to better understand the potential functions of genes (Shi et al., 2021; Yaschenko et al., 2022), and the specific expression of *DREB* genes in roots drew our attention to flavonoids in Tartary buckwheat (Figure 2b, S7). As a result, we screened candidate genes from flavonoids mGWAS and drought GWAS. It turned out that *FtDREB02* mediated the delphinidin biosynthesis of hairy roots in *F. tataricum* and

enhanced drought tolerance in hairy roots of Tartary buckwheat and *Arabidopsis* (Figure 4a-c, 5b-d). The involvement of anthocyanins in plant resistance to drought stress has been reported in many species (Hinojosa-Gómez et al., 2020; Ren et al., 2023). For example, ABA signaling promotes anthocyanin biosynthesis by inducing the expression of *AcUFGT* in *Aristotelia chilensis*, thereby enhancing plant drought resistance (González-Villagra et al., 2019). *MdERF38* responds to drought stress and interacts with *MdMYB1* to target anthocyanin biosynthesis genes in apple (An et al., 2020). We also observed that after *FtDREB02* overexpression in hairy roots and *Arabidopsis*, the antioxidant enzyme content rose, the cell damaged level decreased, and the tolerance to drought was markedly enhanced. Our transgenic Tartary buckwheat hairy root system revealed coordinated upregulation of drought-responsive genes, including the ABA receptor *FtPYR*, cell wall-associated kinase *FtWAK*, and the ROS-scavenging enzyme *FtAPX* (Figure S15, Table S10) (Mittler and Zilinskas, 1994; Santiago et al., 2009; Li et al., 2025). These findings, combined with the established role of anthocyanins in ROS detoxification and abiotic stress protection, support a dual mechanism of *FtDREB02*-mediated drought tolerance: (1) modulation of delphinidin levels for enhanced ROS scavenging capacity, and (2) transcriptional activation of drought-response genes coupled with increased antioxidant enzyme activity. This suggests that *FtDREB02* can be used as a candidate gene with application value in future breeding work. Unlike previous studies that focused on a single stress response, our study showed that *FtDREB02* integrates multiple pathways, including flavonoid biosynthesis and antioxidant defense pathways, to improve plant drought tolerance. This dual role highlights the potential of *FtDREB02* as a candidate gene for breeding drought-resistant buckwheat varieties. However, we observed that after overexpressing *FtDREB02* in *Arabidopsis*, the transgenic lines had shortened vegetative growth, an early onset of reproductive growth, poor anther development, smaller seeds, and lower yield (Figure S16, Table S23). This is in line with the findings of numerous studies, which show that overexpressing the resistance gene can increase the survival rate of plants in unfavorable circumstances while inhibiting its growth and development in favorable ones (Kim et al., 2004; Fujita et al., 2005; Zhang et al., 2020; Li et al., 2021).

To achieve a multi-level response to abiotic stress, induced *DREBs* can control the expression of several target genes with pertinent interaction sites in the promoter (Agarwal et al., 2017; Mei et al., 2022). In this work, we enriched the core sequences contained in the promoters of target genes through DAP-seq, especially the highly enriched DRE elements, and also confirmed that *FtDREB02* promoted the *FtANS* expression by directly binding to the DRE element on the promoter. In fact, since the flavonol content dropped in *FtDREB02* transgenic hairy roots, we also analyzed the key genes in the flavonol biosynthesis pathway. We found that *FtDREB02* significantly inhibited the promoter activity of *FtFLS* and dramatically down-regulate its expression (Figure S17, Table S22). Although a significant down-regulation of *FtF3'5'H* was observed in *FtDREB02* transgenic hairy roots, *FtDREB02* had no significant effect on its promoter in the transactivation assay (Figure S17, Table S22), which may be related to other interacting proteins. It is speculated that *FtDREB02* may prevent the synthesis of flavonols by targeting the *FtFLS* promoter and promote the buildup of naringenin substrates toward anthocyanins. This is contrast with the earlier research showing flavonols could increase plant resilience to drought (Zhang et al., 2021; Yang et al., 2023; Du et al., 2024). Experiments are still needed to confirm whether this conjecture is accurate. While our study primarily elucidates the role of *FtDREB02* in regulating delphinidin biosynthesis, DAP-seq analysis suggests this transcription factor may orchestrate a broader drought response network. Specifically, we identified *FtDREB02* potential regulating established drought-responsive genes including

FtPYR, *FtWAK* and *FtAPX* – all also co-expressed in the WGCNA Blue3 module and upregulated in transgenic hairy roots (Figure S15; Table S10) (Mittler and Zilinskas, 1994; Santiago et al., 2009; Li et al., 2025). These findings position *FtDREB02* as a potential hub integrating flavonoid metabolism with systemic drought adaptation.

In fact, the *Arabidopsis* homolog *DREB2A* has been reported to significantly enhance drought tolerance while inhibiting plant growth, which aligns with the performance of *FtDREB02* in Tartary buckwheat (Liu et al., 1998; Sakuma et al., 2006). The function of *DREB2A* has been characterized in numerous species including rice (Cui et al., 2011), maize (Qin et al., 2007), wheat (Karki et al., 2013), cowpea (Sadhukhan et al., 2014), *Picea wilsonii* (Huang et al., 2024), *Pennisetum glaucum* (Meena et al., 2022), apple (Li et al., 2023), etc. Its overexpression enhances plant tolerance to abiotic stresses, particularly drought and heat (Qin et al., 2008), demonstrating functional conservation of *DREB2A* across species. Although many studies have investigated DREB proteins in relation to metabolites, the regulation of flavonoids by DREB2A remains unclear. Under water deficit conditions, overexpression of *GmDREB2A* alters the metabolic profile in soybean, notably increasing phenylalanine content—the precursor of phenylpropanoid metabolism (Marinho et al., 2019). Compared to drought-sensitive varieties, the drought-tolerant rapeseed 'Saturnin' shows higher expression levels of both *DREB2* and phenylpropanoid pathway genes, along with greater accumulation of flavonoid compounds, suggesting a potential role of *DREB2* and flavonoids in improving plant water deficit tolerance (Lee et al., 2023). In this study, we demonstrate that the buckwheat *FtDREB02* gene not only enhances reactive oxygen species scavenging capacity under drought conditions, but also improves tolerance to water deficit by promoting delphinidin biosynthesis. These findings provide new insights into the functional characteristics of DREB2 in plants. In conclusion, this study has expanded our knowledge of the genetic evolution of the DREB family in buckwheat species and deepened our understanding of the impact of buckwheat *DREB* genes on delphinidin synthesis and plant drought resistance. In addition, it also provided excellent genetic resources for breeding new buckwheat varieties with abundant active substances and strong drought resistance.

MATERIALS AND METHODS

Genome-wide identification of the *DREB* genes in three buckwheat species

AtDREBs genes were used to identify candidate *DREB* genes via BLASTP search with an E-value of 1×10^{-5} using the whole genome database from *F. dibotrys, F. esculentum* and *F. tataricum* (Zhang et al., 2017; He et al., 2022; Lin et al., 2023). The Hidden Markov Model (HMM) profile of the AP2 domain (PF00847), obtained from the protein family database (Pfam) (http://pfam.xfam.org/), was used to identify *DREB* gene members in buckwheat species using the HMM search function within ToolKit Biologists Tools (TBtools) software (https://github.com/CJ-Chen/TBtools). These candidate proteins were retrieved from both NCBI Conserved Domain Database (https://www.ncbi.nlm.nih.gov/cdd/) and Interpro database (https://www.ebi.ac.uk/interpro/) to confirm the presence of the AP2 domain and key amino acids within their sequences. The confirmed *DREB* genes were renamed according to their positions on chromosomes. The physicochemical properties – protein length, transmembrane structures, topology, molecular weight (MW), and isoelectric point (pI), were assessed by TMHMM 2.0 - DTU Health Tech - Bioinformatic Services (TMHMM , https://services.healthtech.dtu.dk/services/TMHMM-2.0/), and the ExPASy Prot-Param tool (https://web.expasy.org/compute_pi/), respectively. Finally, the subcellular localization of the

protein was determined by the WoLF PSORT (https://wolfpsort.hgc.jp/).

Multiple sequence alignment, conserved domain analysis, and phylogenetic tree construction

The TAIR database (https://www.arabidopsis.org/) provided the genome-wide data of *Arabidopsis* (Huala, 2001). MEGA7.0 was used to perform multiple sequence alignment and build the phylogenetic tree using maximum likelihood (ML) with the Poisson model, and Genedoc3.2 was used to show the outcomes. The AlphaFold protein structure database (https://alphafold.ebi.ac.uk/entry/Q9SVX5) provided the three-dimensional structure of the conserved domain of AP2. The DREBs conserved sequence was visualized with the online website Weblogo 3 (https://weblogo.threeplusone.com/create.cgi). The 3-D structure of *FtDREB02* was predicted online via Alphfold 3 (https://golgi.sandbox.google.com/) and visualized with Discovery software.

Gene structure, motif, and cis-element analysis of DREB family

Multiple Em for Motif Elicitation (MEME, https://meme-suite.org/meme/) and NCBI CDD search (https://www.ncbi.nlm.nih.gov/Structure/bwrpsb/bwrpsb.cgi) were employed to predict conservative motifs and conservative domains, respectively. Plantcare (https://bioinformatics.psb.ugent.be/webtools/plantcare/html/) was used to predict promoter (default is 2kb upstream of the transcription start site (TSS)) elements in plant. TBtools facilitated the visualization of these results (Chen et al., 2020).

Analysis of gene expression in different tissues and under 20% PEG 6000 treatment.

Transcriptome datasets of *F. dibotrys*, *F. esculentum*, and *F. tataricum* were downloaded from NCBI (Hou et al., 2021; Huang et al., 2021; He et al., 2022; Lin et al., 2023). Tissues for Tartary buckwheat were sampled during grain-filling phase under field conditions (Shanxi, 34°36′N) (Hou et al., 2021); Golden buckwheat was collected in Changping base, Beijing in mid-July (He et al., 2022); Commen buckwheat represent standard tissue from greenhouse-grown plants in Sichuan University of Chengdu (Lin et al., 2023). The *DREBs* expression profiles were then visualized, and the $\log_2$ scale was chosen for analysis using TBtools. Cluster analysis was performed using Rstudio software with default settings for 10 cluster according to predecessors (He et al., 2024).

Co-expression networks were constructed using the WGCNA package (v1.73) in R following established methodologies (Langfelder & Horvath, 2008). Briefly, a soft-thresholding power (β) of 18 was selected based on scale-free topology criterion ($R^2 > 0.8$) to construct an adjacency matrix. Topological overlap matrix (TOM) was then generated to measure network interconnectedness, with modules identified using dynamic tree cutting (minimum module size = 50 genes). Module-trait associations were calculated by correlating module eigengenes with phenotypic traits ($P < 0.05$). The gene of interest, *FtDREB02*, was extracted as the first principal component for downstream analysis.

GWAS analysis

GWAS (and mGWAS) were conducted to identify genomic loci and metabolic traits associated with drought resistance in plants. The analysis included 10x and 30x genome resequencing data, expression profiles of key metabolites, and phenotypic traits from Tartary buckwheat (Zhang et al., 2021; Zhao et al., 2023; Lai et al., 2024; He et al., 2024). Association analysis was performed using the Efficient Mixed-Model Association eXpedited program (EMMAx) and factored spectrally transformed linear mixed models (FaST-LMM).

Quantitative real-time PCR analysis

RNA extraction was performed using RNA Easy Fast Plant Tissue RNA Extraction Kit (DP452,

Tiangen) according to the manufacturer's instructions. Reverse transcription reactions were carried out using the HiScriptIII 1st Strand cDNA Synthesis Kit (+gDNA wiper) (R323-01, Vazyme). qRT–PCR was performed using the ChamQ Universal SYBR qPCR Master Mix (Q711-02, Vazyme) following the manufacturer's protocol. Three independent RNA samples were used as biological replicates for each target gene analysis. The Ct values obtained from the qRT-PCR reactions were analyzed using the $2^{-(\Delta\Delta Ct)}$ method. For specific primer sequences, details are provided in Table S24.

Gene clone and transgenic hairy roots of Tartary buckwheat and *Arabidopsis* generation

The *FtDREB02* fragment was amplified from the cDNA of 'PinKu' using specific primers and cloned into the pCAMBIA1307-MYC vector via BamHI and HindIII restriction sites, and subsequently transformed into *Arabidopsis* (Columbia-0) and hairy roots explants of Tartary buckwheat by agrobacterium infection (Clough and Bent, 1998; Zhang et al., 2018; Li et al., 2019). pGreen 0029-GFP was used to construct the subcellular localization vector with EcoRI and XmaI sites. Specific primers are shown in Table S24.

Subcellular localization

The GV3101 monoclone containing fluorescence markers 35S::GFP: *FtDREB02* and NLS-mCherry was propagated in LB medium (containing 50ug/ml rifamycin and 100ug/ml kanamycin) until an optical density on OD_{600}=0.8-1.2 at 37℃, with rotational speed of 220 r/min. Collecting the bacteria by centrifugation, resuspend the pellet with MES suspension (10 mmol/L MES+10 mmol/L $MgCl_2$+200 umol/L acetosyringone), centrifugated and discard the supernatant, repeated twice. The bacterial pellet was resuspended at an optical density of OD600=0.6-0.8, stored in the dark for 1-2 hours. *Nicotiana benthamiana* of 4-6 weeks was used for agrobacterium injection. The plants were cultured in the dark at 25℃ for 24 hours and then transferred to light/dark cycles (16h/8h) for 48 hours. The fluorescence signal was observed using a laser scanning confocal fluorescence microscope 900 (ZEISS). See Table S24 for primer design.

Drought treatment with *Arabidopsis* and hair root of Tartary buckwheat

Arabidopsis seeds were planted on sterilized 1/2 MS plates containing either 150 mM mannitol or no mannitol, placed in a growth chamber at 4°C for 2-3 days and then transfer to standard growth conditions (25°C). After 7 days, seed germination was monitored and counted. There were 4 lines on each plate (1 WT line + 3 OE lines), 27 full seeds were used for each line, at least 5 plates were used for each experiment, and the experiment was repeated three times.

Arabidopsis seedlings grown on 1/2 MS plates for 3-5 days were transferred vertically onto new 1/2 MS plates with or without 150 mM mannitol. The medium was prepared in advance to ensure consistent growth conditions. *Arabidopsis* root length was measured after 1-2 weeks. There were 4 lines on each plate (1 WT line + 3 OE lines), and each line used 3 newly germinated seedlings with consistent growth and root length. There were at least 10 plates for each experiment, and the experiment was repeated three times.

After 10 days of germination on 1/2 MS plates, *Arabidopsis* seedlings were transferred to soil and then placed in standard growth conditions (25°C , 16 h light/8 h dark, 60-80% relative humidity). After 3 weeks of soil growth, plants were thoroughly watered, and drought stress was initiated by withholding water for up to 2 weeks. Phenotypic changes, such as visible wilting, leaf curling, and chlorosis, were monitored daily. Samples were collected when most plants displayed clear wilting symptoms. No rewatering was performed prior to sampling.

Two-centimeter-long Tartary buckwheat hairy roots with consistent growth were cultured in

MS liquid medium supplemented with or without 20% PEG 6000. After a 30 days growth period at standard conditions (25°C, 120 rpm), samples were collected for gene (*FtDREB02*, *FtANS*, *FtFLS*, *FtF3'5'H*) expression detection, fresh weight, LC-MS and physiological measurement.

Hydroponically-grown Tartary buckwheat (*F. tataricum,* cultivated variety 'PinKu') seedlings were maintained for 7 days under controlled conditions (25°C, 16-h-light/8-h-dark photoperiod). Uniform seedlings were selected and treated with 20% (w/v) PEG-6000 solution. Plant samples were collected at 0, 1, 3 and 6 h post-treatment, immediately flash-frozen in liquid nitrogen for subsequent gene (*FtDREB02*, *FtPYR*, *FtWAK*, *FtAPX*) expression detection, and stored at -80°C. Three biological replicates were analyzed per time point.

Metabolites detection

The qPCR analyses (Figure 7d-e) and HPLC-based delphinidin measurements (Table S12) were performed using aliquots from the same biological samples (n=3 independent transgenic events). The extraction and analysis of metabolites from hair root samples were performed under the same experimental methods as previous studies (Zhang et al., 2021; Gao et al., 2025). Each sample was prepared as follows: the fresh material was placed at 65°C overnight, and then grinded. 0.1 g of powder was weighted and dissolved in 10 mL of 80% methanol. Following ultrasound assisted extraction at 40°C for 45 minutes with 40 kHz, the samples were filtered through an 0.22 um organic microporous membrane before LC-MS analysis (Agilent G6500 series HPLC-QQQ). Each sample had three independent biological replicates.

Tartary buckwheat seeds were ground into a fine powder using a mortar. Exactly 0.1 g of the powder was weighed into a 15 ml centrifuge tube and dissolved in 10 ml of 80% methanol. Extraction was assisted by sonication, with all specific parameters and subsequent steps being consistent with those described above. Three independent biological replicates were performed for each germplasm.

Physiological measurements

0.1 g of fresh sample was weighed and placed in a 2 ml EP tube, quickly frozen in liquid nitrogen, and ground into powder. The contents of MDA (BC0025, Solarbio), CAT (BC0205, Solarbio), POD (BC0095, Solarbio) and SOD (BC0175, Solarbio) were determined following the manufacturer's protocol. DAB and NBT staining were performed according to the manual of Nitroblue Tetrazolium Chloride (CN7731, Coolaber) and 3'3-diaminobenzidine tetrahydrochloride (CD4181, Coolaber).

Dual luciferase assay

2kb promoter regions of genes (*FtANS*, *FtFLS*, and *FtF3'5'H*) were amplified via PCR and cloned into the pGreenII 0800-LUC vector, while the CDS of *FtDREB02* was inserted into the pGreenII 62-sk plasmid. Transcriptional activation analysis was performed using *N. benthamiana* leaves. The Renilla luciferase (REN) gene was used as an internal normalization control, with LUC/REN ratio measurements performed under triplicate biological conditions. Detailed primer sequences are provided in Table S24.

Electrophoretic mobility shift assay (EMSA)

The CDS sequence of *FtDREB02* was cloned into the Puc57-Halo vector and expressed protein as described previously (Song et al., 2024). Biotin-labeled probes were designed based on the *FtANS* promoter, and the experiment was performed using the LightShift EMSA kit (Thermo Fisher Scientific, Waltham, MA, USA). The specific probe sequences are listed in Table S24.

DAP-seq data analysis

DAP-seq experiments were performed according to previously described protocols (Li et al., 2023). Sequencing technology was provided by Annoroad Gene Technology (China). Peak calling was processed using bedtools bamtobed (Quinlan and Hall, 2010), followed by macs2 normalization (Zhang et al., 2008). Peaks were associated with the nearest gene model in the *F. tataricum* genome annotation file using the BioConductor package ChIPseeker under default parameters (Yu et al., 2015). HOMER was used for motif discovery (Heinz et al., 2010).

KEGG analysis

KEGG pathway enrichment analysis was performed using the OmicShare server (https://www.omicshare.com/) and default parameters. The input gene list was tested against the fully annotated genome background using Fisher's exact probability method, and the resulting p-values were corrected using the Benjamini-Hochberg method. Pathways with FDR < 0.05 were considered significantly enriched.

Virus-induced gene silencing (VIGS) assay

For VIGS construct preparation, a 300-bp gene-specific fragment was amplified using primers *Ftdreb02*-F/R (Table S24) and subsequently cloned into the pTRV2 vector to generate the recombinant pTRV2-*Ftdreb02* plasmid. The empty vectors (pTRV1 and pTRV2) along with the recombinant pTRV2-*Ftdreb02* were individually transformed into strain GV3101. Positive clones were selected and cultured to an OD600=0.8-1.0, then resuspended in infiltration buffer to adjust the OD600=0.8. Equal volumes of pTRV1 and either pTRV2 or pTRV2-*Ftdreb02* suspensions were mixed and incubated in darkness for 2 h prior to plant infection. Surface-sterilized buckwheat seeds were carefully decoated and immersed in the bacterial suspension, followed by gentle agitation on a rotary shaker for 20-30 min. After infection, seeds were rinsed 5-6 times with sterile water, placed on moist filter paper, and maintained in darkness for 48 h before transfer to standard growth conditions (16-h light/8-h dark photoperiod at 25°C).

To assess silencing efficiency, randomly selected 12-day-old seedlings were subjected to gene expression analysis. Subsequently, 13-15-day-old seedlings were measured for delphinidin content using previously described methods and treated with 20% PEG-6000 for 6 h to impose osmotic stress. All experiments were performed with three biological replicates, with each replicate containing at least 10 individual plants per treatment group.

Statistics

GraphPad Prism 10.1.2 software was used to conduct the anova analysis and student t-tests of variance. Quantitative data are expressed as mean ± SD from triplicate biological experiments (n = 3 at least), with statistical significance indicated by asterisks (*P< 0.05, **P < 0.01, ***P < 0.001).

AUTHOR CONTRIBUTIONS

The work was conceived and designed by MZ, MLF, GP, and KZ. JW, DF, YS, XW, and HL conducted the experiments and data analysis. The manuscript was written by JW, CG, YH, and RJ. The manuscript was revised by MLF, GP, MQ, KZ, and MZ. The published version of the manuscript has been read and approved by all authors.

ACKNOWLEDGMENTS

This research was supported by National Key Research and Development Program of China (2022YFE0140800) and National High-level University Graduate Scholarship Program of the China Scholarship Council (202303250057).

CONFLICT OF INTEREST STATEMENT

No conflicting interests are declared by all the authors.

DATA AVAILABILITY STATEMENT

20% PEG 6000 transcriptome of F. tataricum was retrieved from the China National Center for Bioinformation Genome Sequence Archive (accession number: PRJCA003569). DAP-seq data generated in this study have been submitted to China National Center for Bioinformation Genome Sequence Archive (accession number: PRJCA043178).

SUPPORTING INFORMATION

All Supporting Information may be found in the main text or the supplementary details.

Figure S1 Sequence alignment of DREB proteins in *Fagopyrum dibotrys*, *Fagopyrum tataricum*, and *Fagopyrum esculentum*.

Figure S2 Sequence logo of conserved amino acids in DREBs protein. (a)FdDREBs. (b) FeDREBs.

Figure S3 Chromosomal distribution of *DREBs.* Chromosomal distribution of *FdDREBs* (a), *FeDREBs* (b), and *FtDREBs* (c).

Figure S4 *DREB* genes duplication events in buckwheat species. (a) *Fagopyrum dibotrys*. (b) *Fagopyrum esculentum*. (c) *Fagopyrum tataricum.*

Figure S5 Venn diagram of collinearity gene pairs between *F. dibotrys* vs. *F. esculentum* and *F. dibotrys* vs. *F. tataricum*.Figure S6 Phylogenetic relationships, gene structure, the conserved protein motifs, and CREs of DREBs. (a) in *F. dibotrys*. (b) in *F. esculentum*. (c) in *F. tataricum*.

Figure S7 Expression patterns of *DREB* genes in different tissues. (a) in *F. dibotrys*. (b) in *F. esculentum*.

Figure S8 mGWAS for delphinidin. (a)10x and (b) 30x mGWAS Manhattan plot of delphinidin content. (c) 10x and (d) 30x QQ-plot for delphinidin mGWAS.

Figure S9 Transcriptome heat map of GWAS co-localized genes under 20% PEG stress. The gradient color scale from olive green (Hex: #006666) to saddle brown (Hex: #993300) indicates the continuum of gene expression levels, with light green representing low expression (normalized log2FC$\leqslant$-1) and dark brown denoting high expression (normalized log2FC$\geqslant$1).

Figure S10 Sequence alignment of *FtDREB02* homologous genes within three buckwheat species. (a) *F. dibotrys* (b) *F. esculentum* (c) *F. tataricum.*

Figure S11. Virus-induced gene silencing of *FtDREB02* in Tartary buckwheat seedlings. (a) Relative expression levels of *FtDREB02* in silenced lines (dreb1, dreb2, and dreb3) compared with control plants. (b) Delphinidin content in negative control and silenced lines. (c) Phenotypic characteristics of negative control and silenced lines after 6 hours of 20% PEG-6000 osmotic stress treatment. (d) DAB staining of Tartary buckwheat seedlings following osmotic stress exposure. Data represent mean ± SD from at least three independent biological replicates for each group. Statistical significance was determined by Student's t-test ($P < 0.05$, *$P < 0.01$, ***$P < 0.0001$).

Figure S12 Seed germination of *Arabidopsis* under normal MS conditions and 150 mM mannitol treatment. Data represent mean ± SD from at least three independent biological replicates for each group. Statistical significance was determined by Student's t-test ($P < 0.05$, *$P < 0.01$, ***$P < 0.0001$).

Figure S13 DAB and NBT staining of *Arabidopsis* leaves after natural drought stress. The black bar is 1 cm.

Figure S14 Subcellular localization of *FtDREB02.*

Figure S15 Drought-responsive gene expression in FtDREB02-overexpressing hairy roots. Data

represent mean ± SD from at least three independent biological replicates for each group. Statistical significance was determined by Student's t-test ($P < 0.05$, *$P < 0.01$, ***$P < 0.0001$).

Figure S16 Phenotypic changes of *FtDREB02* overexpression in *Arabidopsis*. (a) Differences in growth and development between Col-0 and *FtDREB02*-OE lines under normal growth conditions. (b-c) The seeds phenotype of Col-0 and *FtDREB02*-OE lines grown in normal conditions. Black bar is 0.5 cm. (d-f) Seed length, width and hundred grain weight of Col-0 and *FtDREB02*-OE lines as described in (b-c). Data represent mean ± SD from at least three independent biological replicates for each group. Statistical significance was determined by Student's t-test ($P < 0.05$, *$P < 0.01$, ***$P < 0.0001$).

Figure S17 The effect of *FtDREB02* on *FtFLS* and *FtF3'5'H*. The relative expression of *FtFLS* (a) and *FtF3'5'H* (b) in A4 control lines and OE-*FtDREB02* hair root. (c-e) Measurement firefly luciferase (LUC) and renilla luciferase (REN) activitie. Data represent mean ± SD from at least three independent biological replicates for each group. Statistical significance was determined by Student's t-test ($P < 0.05$, *$P < 0.01$, ***$P < 0.0001$).

Table S1 Basic information of the DREBs in buckwheat.

Table S2 Collinear gene pairs and duplications types of *DREBs* in buckwheat.

Table S3 Information of motifs identified from DREB proteins in buckwheat.

Table S4 CREs in the 2kb promoter of DREBs gene in buckwheat.

Table S5 The number and proportion of genes with the highest expression in each tissue.

Table S6 Phenotypic data for mGWAS and drought GWAS analysis (Zhao et al., 2023; He et al., 2024).

Table S7 Candidate genes determined by GWAS.

Table S8 PlantPAN4.0 prediction results of variation sites of *FtDREB02* promoter.

Table S9 Delphinidin content in three buckwheat species。

Table S10 Relative expression of *FtDREB02* under 20% PEG treatment and drought-related gene in OE-*FtDREB02* hairy root.

Table S11 Genes of the blue3 module based on PEG transcriptome.

Table S12 Metabolites content in hairy root of overexpression *FtDREB02* in *F. tataricum*.

Table S13 Biomass and physiological index in hairy root under MS and 20% PEG treantment condition.

Table S14 Relative gene expression level of *FtDREB02* and delphinidin content in virus-induced gene silencing strains.

Table S15 Seed germination rate under normal 1/2MS culture and 150mM mannitol in *Arabidopsis thaliana*.

Table S16 Root length (cm) under normal 1/2MS culture and 150mM mannitol in *Arabidopsis thaliana*.

Table S17 Survival rate and physiological index in *A. thaliana* under natural drought.

Table S18 Information of DAP-seq binding peaks after excluding controls.

Table S19 KEGG enrichment analysis results of genes with DAP-seq binding peaks located in the 2kb promoter region.

Table S20 Cluster analysis of PEG transcriptome.

Table S21 LUC/REN of D-luciferase reporter gene assay.

Table S22 Relative expression of genes in *FtDREB02* transgenic hairy roots.

Table S23 Seed length, width, and 100 grain weight of *Arabidopsis*.

Table S24 Specific primer sequence.

[dataset]REFERENCES

An, J.P., Zhang, X.W., Bi, S.Q., You, C.X., Wang, X.F., Hao, Y.J. (2020) The ERF transcription factor MdERF38 promotes drought stress-induced anthocyanin biosynthesis in apple. Plant J, 101, 573–589. https://doi.org/10.1111/tpj.14555

Ayyoub, A., Yu, X., Zhang, X., Gao, C., Li, J., Yin, S., Chen, S., Liesche, J. (2024) Drought-dependent regulation of cell coupling in Arabidopsis leaf epidermis requires plasmodesmal protein NHL12. J. Exp. Bot. 75, 7019–7030. https://doi.org/10.1093/jxb/erae370

Bagal, D., Chowdhary, A.A., Mehrotra, S., Mishra, S., Rathore, S., Srivastava, V. (2023) Metabolic engineering in hairy roots: An outlook on production of plant secondary metabolites. Plant Physiol. Biochem. 201, 107847. https://doi.org/10.1016/j.plaphy.2023.107847**Bailey-Serres, J., Parker, J.E., Ainsworth, E.A., Oldroyd, G.E.D., Schroeder, J.I.** (2019) Genetic strategies for improving crop yields. Nature, 575, 109–118. https://doi.org/10.1038/s41586-019-1679-0

Cella Pizarro, L., Bisigato, A.J. (2010) Allocation of biomass and photoassimilates in juvenile plants of six Patagonian species in response to five water supply regimes. Ann. Bot, 106, 297–307. https://doi.org/10.1093/aob/mcq109

Chen, C., Chen, H., Zhang, Y., Thomas, H.R., Frank, M.H., He, Y., Xia, R. (2020) TBtools: an integrative toolkit developed for interactive analyses of big biological data. Mol. Plant, 13, 1194–1202. https://doi.org/10.1016/j.molp.2020.06.009

Clough, S.J., Bent, A.F. (1998) Floral dip: a simplified method for Agrobacterium-mediated transformation of *Arabidopsis thaliana*. Plant J, 16, 735–743. https://doi.org/10.1046/j.1365-313x.1998.00343.x

Cui, M., Zhang, W., Zhang, Q., Xu, Z., Zhu, Z., Duan, F., Wu, R. (2011) Induced over-expression of the transcription factor OsDREB2A improves drought tolerance in rice. Plant Physiol. Biochem. PPB 49, 1384–1391. https://doi.org/10.1016/j.plaphy.2011.09.012

Faize, M., Burgos, L., Faize, L., Piqueras, A., Nicolas, E., Barba-Espin, G., Clemente-Moreno, M.J., Alcobendas, R., Artlip, T., Hernandez, J.A. (2011) Involvement of cytosolic ascorbate peroxidase and Cu/Zn-superoxide dismutase for improved tolerance against drought stress. J. Exp. Bot. 62, 2599–2613. https://doi.org/10.1093/jxb/erq432**Fang, Z.W., Xu, X.Y., Gao, J.F., Wang, P.K., Liu, Z.X., Feng, B.L.** (2015) Characterization of *FeDREB1* promoter involved in cold- and drought-inducible expression from common buckwheat (*Fagopyrum esculentum*). Genet. Mol. Res, 14, 7990–8000. https://doi.org/10.4238/2015.July.17.7

Flagel, L.E., Wendel, J.F. (2009) Gene duplication and evolutionary novelty in plants. New Phytol, 183, 557–564. https://doi.org/10.1111/j.1469-8137.2009.02923.x

Fujita, Y., Fujita, M., Satoh, R., Maruyama, K., Parvez, M.M., Seki, M., Hiratsu, K., Ohme-Takagi, M., Shinozaki, K., Yamaguchi-Shinozaki, K. (2005) AREB1 is a transcription activator of novel ABRE-dependent ABA signaling that enhances drought stress tolerance in *Arabidopsis*. Plant Cell, 17, 3470–3488. https://doi.org/10.1105/tpc.105.035659

Gao, L.-L., Xue, H.-W. (2012) Global Analysis of Expression Profiles of Rice Receptor-Like Kinase Genes. Mol. Plant 5, 143–153. https://doi.org/10.1093/mp/ssr062**Gahlaut, V., Jaiswal, V., Kumar, A., Gupta, P.K.** (2016) Transcription factors involved in drought tolerance and their possible role in developing drought tolerant cultivars with emphasis on wheat (*Triticum aestivum L.*). Theor. Appl. Genet, 129, 2019–2042. https://doi.org/10.1007/s00122-016-2794-z

Gao, Y., Shi, Y., Jahan, T., Huda, Md.N., Hao, L., He, Y., Quinet, M., Chen, H., Zhang, K., Zhou,

M. (2025) Buckwheat UDP-glycosyltransferase *FtUGT71K6* and *FtUGT71K7* tandem repeats contribute to drought tolerance by regulating epicatechin synthesis. Plant Cell Environ, https://doi.org/10.1111/pce.15412

Georgiev, M.I., Pavlov, A.I., Bley, T. (2007) Hairy root type plant in vitro systems as sources of bioactive substances. Appl. Microbiol. Biotechnol. 74, 1175–1185. https://doi.org/10.1007/s00253-007-0856-5

Giri, A., Narasu, M.L. (2000) Transgenic hairy roots. recent trends and applications. Biotechnol. Adv. 18, 1 – 22. https://doi.org/10.1016/s0734-9750(99)00016-6**González-Villagra, J., Cohen, J.D., Reyes-Díaz, M.M.** (2019) Abscisic acid is involved in phenolic compounds biosynthesis, mainly anthocyanins, in leaves of *Aristotelia chilensis* plants (Mol.) subjected to drought stress. Physiol. Plant, 165, 855–866. https://doi.org/10.1111/ppl.12789

Guillon, S., Trémouillaux-Guiller, J., Pati, P.K., Rideau, M., Gantet, P. (2006) Hairy root research: recent scenario and exciting prospects. Curr. Opin. Plant Biol., Physiology and metabolism / edited by Eran Pichersky and Krishna Niyogi 9, 341–346. https://doi.org/10.1016/j.pbi.2006.03.008**Guo, F., Guan, R., Sun, X., Zhang, C., Shan, C., Liu, M., Cui, N., Wang, P., Lin, H.** (2023) Integrated metabolome and transcriptome analyses of anthocyanin biosynthesis reveal key candidate genes involved in colour variation of *Scutellaria baicalensis* flowers. BMC Plant Biol, 23, 643. https://doi.org/10.1186/s12870-023-04591-3

He, J., Hao, Y., He, Y., Li, W., Shi, Y., Khurshid, M., Lai, D., Ma, C., Wang, X., Li, J., Cheng, J., Fernie, A.R., Ruan, J., Zhang, K., Zhou, M. (2024) Genome-wide associated study identifies *FtPMEI13* gene conferring drought resistance in Tartary buckwheat. Plant J, 120, 2398–2419. https://doi.org/10.1111/tpj.17119

He, M., He, Y., Zhang, K., Lu, X., Zhang, X., Gao, B., Fan, Y., Zhao, H., Jha, R., Huda, Md.N., Tang, Y., Wang, J., Yang, W., Yan, M., Cheng, J., Ruan, J., Dulloo, E., Zhang, Z., Georgiev, M.I., Chapman, M.A., Zhou, M. (2022) Comparison of buckwheat genomes reveals the genetic basis of metabolomic divergence and ecotype differentiation. New Phytol, 235, 1927–1943. https://doi.org/10.1111/nph.18306

Heinz, S., Benner, C., Spann, N., Bertolino, E., Lin, Y.C., Laslo, P., Cheng, J.X., Murre, C., Singh, H., Glass, C.K. (2010) Simple combinations of lineage-determining transcription factors prime *cis*-regulatory elements required for macrophage and B cell identities. Mol. Cell, 38, 576–589. https://doi.org/10.1016/j.molcel.2010.05.004

Hinojosa-Gómez, J., San Martín-Hernández, C., Heredia, J.B., León-Félix, J., Osuna-Enciso, T., Muy-Rangel, M.D. (2020) Anthocyanin induction by drought stress in the calyx of roselle cultivars. Mol. Basel Switz, 25, 1555. https://doi.org/10.3390/molecules25071555

Hou, S.Y., Du, W., Hao, Y.R., Han, Y.H., Li, H.Y., Liu, L.L., Zhang, K.X., Zhou, M.L., Sun, Z.X. (2021) Elucidation of the regulatory network of flavonoid biosynthesis by profiling the metabolome and transcriptome in Tartary buckwheat. J Agric Food Chem, 69, 7218-7229. doi: 10.1021/acs.jafc.1c00190

Hu, X., Liang, J., Wang, W., Cai, C., Ye, S., Wang, N., Han, F., Wu, Y., Zhu, Q. (2023) Comprehensive genome-wide analysis of the *DREB* gene family in Moso bamboo (*Phyllostachys edulis*): evidence for the role of *PeDREB28* in plant abiotic stress response. Plant J, 116, 1248–1270. https://doi.org/10.1111/tpj.16420

Hu, Y., Chen, X., Shen, X. (2022) Regulatory network established by transcription factors transmits drought stress signals in plant. Stress Biol, 2, 26. https://doi.org/10.1007/s44154-022-00048-z

Huala, E. (2001) The Arabidopsis Information Resource (TAIR): a comprehensive database and web-based information retrieval, analysis, and visualization system for a model plant. Nucleic Acids Res, 29, 102–105. https://doi.org/10.1093/nar/29.1.102

Huang, J., Chen, Q, Rong, Y., Tang, B., Zhu, L., Ren, R., Shi, T., Chen, Q. (2021) Transcriptome analysis revealed gene regulatory network involved in PEG-induced drought stress in Tartary buckwheat (*Fagopyrum Tararicum*). PeerJ, 9, e11136. https://doi.org/10.7717/peerj.11136

Huang, Y., Du, B., Yu, M., Cao, Y., Liang, K., Zhang, L. (2024) Picea wilsonii NAC31 and DREB2A Cooperatively Activate ERD1 to Modulate Drought Resistance in Transgenic Arabidopsis. Int. J. Mol. Sci. 25, 2037. https://doi.org/10.3390/ijms25042037

Hu, Z.-B., Du, M. (2006) Hairy Root and Its Application in Plant Genetic Engineering. J. Integr. Plant Biol. 48, 121–127. https://doi.org/10.1111/j.1744-7909.2006.00121.

Jedličková, V., Štefková, M., Mandáková, T., Sánchez López, J.F., Sedláček, M., Lysak, M.A., Robert, H.S. (2024) Injection-based hairy root induction and plant regeneration techniques in Brassicaceae. Plant Methods 20, 29. https://doi.org/10.1186/s13007-024-01150-1**Jha, R., Zhang, K., He, Y., Mendler-Drienyovszki, N., Magyar-Tábori, K., Quinet, M., Germ, M., Kreft, I., Meglič, V., Ikeda, K., Chapman, M.A., Janovská, D., Podolska, G., Woo, S.-H., Bruno, S., Georgiev, M.I., Chrungoo, N., Betekhtin, A., Zhou, M.** (2024) Global nutritional challenges and opportunities: buckwheat, a potential bridge between nutrient deficiency and food security. Trends Food Sci. Technol, 145, 104365. https://doi.org/10.1016/j.tifs.2024.104365

Jogawat, A., Yadav, B., Chhaya, Lakra, N., Singh, A.K., Narayan, O.P. (2021) Crosstalk between phytohormones and secondary metabolites in the drought stress tolerance of crop plants: A review. Physiol. Plant, 172, 1106–1132. https://doi.org/10.1111/ppl.13328

Karki, A., Horvath, D.P., Sutton, F. (2013) Induction of DREB2A pathway with repression of E2F, jasmonic acid biosynthetic and photosynthesis pathways in cold acclimation-specific freeze-resistant wheat crown. Funct. Integr. Genomics 13, 57 – 65. https://doi.org/10.1007/s10142-012-0303-2**Kershaw, K.A., Levitt, J.** (1973) Responses of plants to environmental stresses. The Bryologist, 76, 328. https://doi.org/10.2307/3241344

Kumar, S., Muthuvel, J., Sadhukhan, A., Kobayashi, Y., Koyama, H., Sahoo, L. (2022) Enhanced osmotic adjustment, antioxidant defense, and photosynthesis efficiency under drought and heat stress of transgenic cowpea overexpressing an engineered DREB transcription factor. Plant Physiol, Biochem, 193, 1–13. https://doi.org/10.1016/j.plaphy.2022.09.028

Langfelder, P., Horvath, S. (200) WGCNA: an R package for weighted correlation network analysis. BMC Bioinformatics 9, 559. https://doi.org/10.1186/1471-2105-9-559

Lee, B.-R., Park, S.-H., Muchlas, M., La, V.H., Al Mamun, M., Bae, D.-W., Kim, T.-H. (2023) Differential response of phenylpropanoid pathway as linked to hormonal change in two Brassica napus cultivars contrasting drought tolerance. Physiol. Plant. 175, e14115. https://doi.org/10.1111/ppl.14115**Li, M., Yao, T., Lin, W., Hinckley, W.E., Galli, M., Muchero, W., Gallavotti, A., Chen, J.-G., Huang, S.C.** (2023) Double DAP-seq uncovered synergistic DNA binding of interacting bZIP transcription factors. Nat. Commun, 14, 2600. https://doi.org/10.1038/s41467-023-38096-2

Li, X.-L., Meng, D., Li, M.-J., Zhou, J., Yang, Y.-Z., Zhou, B.-B., Wei, Q.-P., Zhang, J.-K. (2023) Transcription factors MhDREB2A/MhZAT10 play a role in drought and cold stress response crosstalk in apple. Plant Physiol. 192, 2203–2220. https://doi.org/10.1093/plphys/kiad147

Li, X., Qi, S., Meng, L., Su, P., Sun, Y., Li, N., Wang, D., Fan, Y., Song, Y. (2025) Genome-wide

identification of the wall-associated kinase gene family and their expression patterns under various abiotic stresses in soybean (Glycine max (L.) Merr). Front. Plant Sci. 15. https://doi.org/10.3389/fpls.2024.1511681**Li, Y., Zheng, Y.P., Zhou, X.H., Yang, X.M., He, X.R., Feng, Q., Zhu, Y., Li, G.B., Wang, H., Zhao, J.H., Hu, X.H., Pu, M., Zhou, S.X., Ji, Y.P., Zhao, Z.X., Zhang, J.W., Huang, Y.Y., Fan, J., Zhang, L.L., Wang, W.M.** (2021) Rice miR1432 fine-tunes the balance of yield and blast disease resistance via different modules. Rice, 14, 87. https://doi.org/10.1186/s12284-021-00529-1

Lin, H., Yao, Y.J., Sun, P.C., Feng, L.D., Wang, S., Ren, Y.M., Yu, X., Xi, Z.X., Liu, J. (2023) Haplotype-resolved genomes of two buckwheat crops provide insights into their contrasted rutin concentrations and reproductive systems. BMC Plant Biol, 21, 87. https://doi.org/10.1186/s12915-023-01587-1

Liu, M., Sun, W., Ma, Z., Zheng, T., Huang, L., Wu, Q., Zhao, G., Tang, Z., Bu, T., Li, C., Chen, H. (2019) Genome-wide investigation of the AP2/ERF gene family in Tartary buckwheat (*Fagopyum tataricum*). BMC Plant Biol, 19, 84. https://doi.org/10.1186/s12870-019-1681-6

Liu, T., Chen, T., Kan, J., Yao, Y., Guo, D., Yang, Y., Ling, X., Wang, J., Zhang, B. (2022) The GhMYB36 transcription factor confers resistance to biotic and abiotic stress by enhancing PR1 gene expression in plants. Plant Biotechnol. J. 20, 722–735. https://doi.org/10.1111/pbi.13751

Liu, Q., Kasuga, M., Sakuma, Y., Abe, H., Miura, S., Yamaguchi-Shinozaki, K., Shinozaki, K. (1998) Two transcription factors, DREB1 and DREB2, with an EREBP/AP2 DNA binding domain separate two cellular signal transduction pathways in drought- and low-temperature-responsive gene expression, respectively, in Arabidopsis. Plant Cell 10, 1391–1406. https://doi.org/10.1105/tpc.10.8.1391**Liu, Y., Zhu, Q., Zhu, N.** (2008) Recent duplication and positive selection of the *GAGE* gene family. Genetica, 133, 31–35. https://doi.org/10.1007/s10709-007-9179-9

Magadum, S., Banerjee, U., Murugan, P., Gangapur, D., Ravikesavan, R. (2013) Gene duplication as a major force in evolution. J. Genet, 92, 155–161. https://doi.org/10.1007/s12041-013-0212-8

Májeková, M., Martínková, J., Hájek, T. (2019) Grassland plants show no relationship between leaf drought tolerance and soil moisture affinity, but rapidly adjust to changes in soil moisture. URL https://besjournals.onlinelibrary.wiley.com/doi/10.1111/1365-2435.13312.

Marinho, J.P., Coutinho, I.D., da Fonseca Lameiro, R., Marin, S.R.R., Colnago, L.A., Nakashima, K., Yamaguchi-Shinozaki, K., Nepomuceno, A.L., Mertz-Henning, L.M. (2019) Metabolic alterations in conventional and genetically modified soybean plants with GmDREB2A;2 FL and GmDREB2A;2 CA transcription factors during water deficit. Plant Physiol. Biochem. PPB 140, 122–135. https://doi.org/10.1016/j.plaphy.2019.04.040

Meena, R.P., Ghosh, G., Vishwakarma, H., Padaria, J.C. (2022) Expression of a Pennisetum glaucum gene *DREB2A* confers enhanced heat, drought and salinity tolerance in transgenic Arabidopsis. Mol. Biol. Rep. 49, 7347–7358. https://doi.org/10.1007/s11033-022-07527-6**Mei, F., Chen, B., Du, L., Li, S., Zhu, D., Chen, N., Zhang, Y., Li, F., Wang, Z., Cheng, X., Ding, L., Kang, Z., Mao, H.** (2022) A gain-of-function allele of a DREB transcription factor gene ameliorates drought tolerance in wheat. Plant Cell, 34, 4472–4494. https://doi.org/10.1093/plcell/koac248

Metz, J., Lampei, C., Bäumler, L., Bocherens, H., Dittberner, H., Henneberg, L., de Meaux, J., Tielbörger, K. (2020) Rapid adaptive evolution to drought in a subset of plant traits in a large-scale climate change experiment. Ecol. Lett, 23, 1643–1653. https://doi.org/10.1111/ele.13596

Mittler, R., Zilinskas, B.A. (1994) Regulation of pea cytosolic ascorbate peroxidase and other antioxidant enzymes during the progression of drought stress and following recovery from drought.

Plant J. Cell Mol. Biol. 5, 397–405. https://doi.org/10.1111/j.1365-313x.1994.00397.x

Mokhosoev, I.M., Astakhov, D.V., Terentiev, A.A., Moldogazieva, N.T. (2024) Cytochrome P450 monooxygenase systems: Diversity and plasticity for adaptive stress response. Prog. Biophys. Mol. Biol. 193, 19 – 34. https://doi.org/10.1016/j.pbiomolbio.2024.09.003 **Morran, S., Eini, O., Pyvovarenko, T., Parent, B., Singh, R., Ismagul, A., Eliby, S., Shirley, N., Langridge, P., Lopato, S.** (2011) Improvement of stress tolerance of wheat and barley by modulation of expression of DREB/CBF factors. Plant Biotechnol. J, 9, 230–249. https://doi.org/10.1111/j.1467-7652.2010.00547.x

Muhammad Aslam, M., Waseem, M., Jakada, B.H., Okal, E.J., Lei, Z., Saqib, H.S.A., Yuan, W., Xu, W., Zhang, Q. (2022) Mechanisms of abscisic acid-mediated drought stress responses in plants. Int. J. Mol. Sci, 23, 1084. https://doi.org/10.3390/ijms23031084

Nakabayashi, R., Yonekura-Sakakibara, K., Urano, K., Suzuki, M., Yamada, Y., Nishizawa, T., Matsuda, F., Kojima, M., Sakakibara, H., Shinozaki, K., Michael, A.J., Tohge, T., Yamazaki, M., Saito, K. (2014) Enhancement of oxidative and drought tolerance in *Arabidopsis* by overaccumulation of antioxidant flavonoids. Plant J, 77, 367–379. https://doi.org/10.1111/tpj.12388

Nguyen, D.V., Hoang, T.T.-H., Le, N.T., Tran, H.T., Nguyen, C.X., Moon, Y.-H., Chu, H.H., Do, P.T. (2021) An Efficient Hairy Root System for Validation of Plant Transformation Vector and CRISPR/Cas Construct Activities in Cucumber (Cucumis sativus L.). Front. Plant Sci. 12, 770062. https://doi.org/10.3389/fpls.2021.770062 **Panchy, N., Lehti-Shiu, M., Shiu, S.-H.** (2016) Evolution of gene duplication inplants. Plant Physiol, 171, 2294–2316. https://doi.org/10.1104/pp.16.00523

Qin, F., Kakimoto, M., Sakuma, Y., Maruyama, K., Osakabe, Y., Tran, L.-S.P., Shinozaki, K., Yamaguchi-Shinozaki, K. (2007) Regulation and functional analysis of ZmDREB2A in response to drought and heat stresses in *Zea mays L.* Plant J. Cell Mol. Biol. 50, 54 – 69. https://doi.org/10.1111/j.1365-313X.2007.03034.x

Qin, F., Sakuma, Y., Tran, L.-S.P., Maruyama, K., Kidokoro, S., Fujita, Y., Fujita, M., Umezawa, T., Sawano, Y., Miyazono, K.-I., Tanokura, M., Shinozaki, K., Yamaguchi-Shinozaki, K. (2008) Arabidopsis DREB2A-interacting proteins function as RING E3 ligases and negatively regulate plant drought stress-responsive gene expression. Plant Cell 20, 1693 – 1707. https://doi.org/10.1105/tpc.107.057380

Qin, Yaqi, Wang, D., Fu, J., Zhang, Z., Qin, Yonghua, Hu, G., Zhao, J. (2021) *Agrobacterium rhizogenes*-mediated hairy root transformation as an efficient system for gene function analysis in *Litchi chinensis*. Plant Methods 17, 103. https://doi.org/10.1186/s13007-021-00802-w **Quinlan, A.R., Hall, I.M.** (2010) BEDTools: a flexible suite of utilities for comparing genomic features. Bioinformatics, 26, 841–842. https://doi.org/10.1093/bioinformatics/btq033

Ramasamy, M., Dominguez, M.M., Irigoyen, S., Padilla, C.S., Mandadi, K.K. (2023) *Rhizobium rhizogenes*-mediated hairy root induction and plant regeneration for bioengineering citrus. Plant Biotechnol. J. 21, 1728–1730. https://doi.org/10.1111/pbi.14096 **Reis, R.R., Andrade Dias Brito da Cunha, B., Martins, P.K., Martins, M.T.B., Alekcevetch, J.C., Chalfun-Júnior, A., Andrade, A.C., Ribeiro, A.P., Qin, F., Mizoi, J., Yamaguchi-Shinozaki, K., Nakashima, K., Carvalho, J. de F.C., de Sousa, C.A.F., Nepomuceno, A.L., Kobayashi, A.K., Molinari, H.B.C.** (2014) Induced over-expression of *AtDREB2A CA* improves drought tolerance in sugarcane. Plant Sci, 221–222, 59–68. https://doi.org/10.1016/j.plantsci.2014.02.003

Ren, M., Wang, Z., Xue, M., Wang, X., Zhang, F., Zhang, Y., Zhang, W., Wang, M. (2019)

Constitutive expression of an A-5 subgroup member in the DREB transcription factor subfamily from *Ammopiptanthus mongolicus* enhanced abiotic stress tolerance and anthocyanin accumulation in transgenic *Arabidopsis*. PloS One, 14, e0224296. https://doi.org/10.1371/journal.pone.0224296

Ren, Y., Zhang, S., Zhao, Q., Wu, Y., Li, H. (2023) The *CsMYB123* and *CsbHLH111* are involved in drought stress-induced anthocyanin biosynthesis in *Chaenomeles speciosa*. Mol. Hortic, 3, 25. https://doi.org/10.1186/s43897-023-00071-2

Riechmann, J.L., Meyerowitz, E.M. (1998) The AP2/EREBP family of plant transcription factors. Biol. Chem, 379, 633–654. https://doi.org/10.1515/bchm.1998.379.6.633

Sadhukhan, A., Panda, S.K., Sahoo, L. (2014) The cowpea RING ubiquitin ligase VuDRIP interacts with transcription factor VuDREB2A for regulating abiotic stress responses. Plant Physiol. Biochem. PPB 83, 51–56. https://doi.org/10.1016/j.plaphy.2014.07.007

Sakuma, Y., Maruyama, K., Qin, F., Osakabe, Y., Shinozaki, K., Yamaguchi-Shinozaki, K. (2006) Dual function of an Arabidopsis transcription factor DREB2A in water-stress-responsive and heat-stress-responsive gene expression. Proc. Natl. Acad. Sci. U. S. A. 103, 18822–18827. https://doi.org/10.1073/pnas.0605639103

Santiago, J., Rodrigues, A., Saez, A., Rubio, S., Antoni, R., Dupeux, F., Park, S.-Y., Márquez, J.A., Cutler, S.R., Rodriguez, P.L. (2009) Modulation of drought resistance by the abscisic acid receptor PYL5 through inhibition of clade A PP2Cs. Plant J. 60, 575–588. https://doi.org/10.1111/j.1365-313X.2009.03981.x**Sarkar, T., Thankappan, R., Mishra, G.P., Nawade, B.D.** (2019) Advances in the development and use of DREB for improved abiotic stress tolerance in transgenic crop plants. Physiol. Mol. Biol. Plants, 25, 1323–1334. https://doi.org/10.1007/s12298-019-00711-2

Seth, P., Sebastian, J. (2024) Plants and global warming: challenges and strategies for a warming world. Plant Cell Rep, 43, 27. https://doi.org/10.1007/s00299-023-03083-w

Song, T., Huo, Q., Li, C., Wang, Q., Cheng, L., Qi, W., Ma, Z., Song, R. (2024) The biosynthesis of storage reserves and auxin is coordinated by a hierarchical regulatory network in maize endosperm. New Phytol, 243, 1855–1869. https://doi.org/10.1111/nph.19949

Sun, W., Xu, Z., Song, C., Chen, S. (2022) Herbgenomics: Decipher molecular genetics of medicinal plants. The Innovation 3, 100322. https://doi.org/10.1016/j.xinn.2022.100322

Tarolli, P., Zhao, W. (2023) Drought in agriculture: Preservation, adaptation, migration. Innov. Geosci. 1, 100002–2. https://doi.org/10.59717/j.xinn-geo.2023.100002**Wang, A., Liu, Y., Li, Q., Li, X., Zhang, X., Kong, J., Liu, Z., Yang, Y., Wang, J.** (2023) *FlbZIP12* gene enhances drought tolerance via modulating flavonoid biosynthesis in *Fagopyrum leptopodum*. Front. Plant Sci, 14. https://doi.org/10.3389/fpls.2023.1279468

Wang, Fang, Harindintwali, J.D., Wei, K., Shan, Y., Mi, Z., Costello, M.J., Grunwald, S., Feng, Z., Wang, Faming, Guo, Y., Wu, X., Kumar, P., Kästner, M., Feng, X., Kang, S., Liu, Z., Fu, Y., Zhao, W., Ouyang, C., Shen, J., Wang, H., Chang, S.X., Evans, D.L., Wang, R., Zhu, C., Xiang, L., Rinklebe, J., Du, M., Huang, L., Bai, Z., Li, S., Lal, R., Elsner, M., Wigneron, J.-P., Florindo, F., Jiang, X., Shaheen, S.M., Zhong, X., Bol, R., Vasques, G.M., Li, X., Pfautsch, S., Wang, M., He, X., Agathokleous, E., Du, H., Yan, H., Kengara, F.O., Brahushi, F., Long, X.-E., Pereira, P., Ok, Y.S., Rillig, M.C., Jeppesen, E., Barceló, D., Yan, X., Jiao, N., Han, B., Schäffer, A., Chen, J.M., Zhu, Y., Cheng, H., Amelung, W., Spötl, C., Zhu, J., Tiedje, J.M. (2023) Climate change: Strategies for mitigation and adaptation. Innov. Geosci. 1, 100015 – 37. https://doi.org/10.59717/j.xinn-geo.2023.100015**Wang, Q., Guan, Y., Wu, Y., Chen, H., Chen, F., Chu, C.** (2008) Overexpression of a rice *OsDREB1F* gene increases salt, drought, and low temperature tolerance in both Arabidopsis

and rice. Plant Mol. Biol, 67, 589–602. https://doi.org/10.1007/s11103-008-9340-6

Wang, Z., Yung, W.-S., Gao, Y., Huang, C., Zhao, X., Chen, Y., Li, M.-W., Lam, H.-M. (2024) From phenotyping to genetic mapping: identifying water-stress adaptations in legume root traits. BMC Plant Biol, 24, 749. https://doi.org/10.1186/s12870-024-05477-8

Wei, H., Wang, X., Wang, K., Tang, X., Zhang, N., Si, H. (2024) Transcription factors as molecular switches regulating plant responses to drought stress. Physiol. Plant, 176, e14366. https://doi.org/10.1111/ppl.14366

Wei, T., Deng, K., Liu, D., Gao, Y., Liu, Y., Yang, M., Zhang, L., Zheng, X., Wang, C., Song, W., Chen, C., Zhang, Y. (2016) Ectopic expression of DREB transcription factor, *AtDREB1A*, confers tolerance to drought in transgenic *Salvia miltiorrhiza*. Plant Cell Physiol, 57, 1593–1609. https://doi.org/10.1093/pcp/pcw084

Wen, W., Li, Z., Shao, J., Tang, Y., Zhao, Z., Yang, J., Ding, M., Zhu, X., Zhou, M. (2021) The distribution and sustainable utilization of buckwheat resources under climate change in China. Plants, 10, 2081. https://doi.org/10.3390/plants10102081

Xiong, H., He, H., Chang, Y., Miao, B., Liu, Z., Wang, Q., Dong, F., Xiong, L. (2025) Multiple roles of NAC transcription factors in plant development and stress responses. J. Integr. Plant Biol. 67, 510–538. https://doi.org/10.1111/jipb.13854 **Xu, Y., Hu, W., Song, S., Ye, X., Ding, Z., Liu, J., Wang, Z., Li, J., Hou, X., Xu, B., Jin, Z.** (2023) *MaDREB1F* confers cold and drought stress resistance through common regulation of hormone synthesis and protectant metabolite contents in banana. Hortic. Res, 10, uhac275. https://doi.org/10.1093/hr/uhac275

Yaschenko, A.E., Fenech, M., Mazzoni-Putman, S., Alonso, J.M., Stepanova, A.N. (2022) Deciphering the molecular basis of tissue-specific gene expression in plants: can synthetic biology help? Curr. Opin. Plant Biol, 68, 102241. https://doi.org/10.1016/j.pbi.2022.102241

Yin, J., Slater, L. (2023) Understanding heatwave-drought compound hazards and impacts on socio-ecosystems. Innov. Geosci. 1, 100042–3. https://doi.org/10.59717/j.xinn-geo.2023.100042 **Yu, G., Wang, L.G., He, Q.Y.** (2015) ChIPseeker: an R/Bioconductor package for ChIP peak annotation, comparison and visualization. Bioinformatics, 31, 2382–2383. https://doi.org/10.1093/bioinformatics/btv145

Zhang, H., Zhao, Y., Zhu, J.K. (2020) Thriving under stress: how plants balance growth and the stress response. Dev. Cell, 55, 529–543. https://doi.org/10.1016/j.devcel.2020.10.012

Zhang, K., He, M., Fan, Y., Zhao, H., Gao, B., Yang, K., Li, F., Tang, Y., Gao, Q., Lin, T., Quinet, M., Janovská, D., Meglič, V., Kwiatkowski, J., Romanova, O., Chrungoo, N., Suzuki, T., Luthar, Z., Germ, M., Woo, S.-H., Georgiev, M.I., Zhou, M. (2021) Resequencing of global Tartary buckwheat accessions reveals multiple domestication events and key loci associated with agronomic traits. Genome Biol, 22, 1–17. https://doi.org/10.1186/s13059-020-02217-7

Zhang, K., He, Y., Lu, X., Shi, Y., Zhao, H., Li, X., Li, J., Liu, Y., Ouyang, Y., Tang, Y., Ren, X., Zhang, X., Yang, W., Sun, Z., Zhang, C., Quinet, M., Luthar, Z., Germ, M., Kreft, I., Janovská, D., Meglič, V., Pipan, B., Georgiev, M.I., Studer, B., Chapman, M.A., Zhou, M. (2023) Comparative and population genomics of buckwheat species reveal key determinants of flavor and fertility. Mol. Plant 16, 1427–1444. https://doi.org/10.1016/j.molp.2023.08.013 **Zhang, L., Li, X., Ma, B., Gao, Q., Du, H., Han, Y., Li, Y., Cao, Y., Qi, M., Zhu, Y., Lu, H., Ma, M., Liu, L., Zhou, J., Nan, C., Qin, Y., Wang, J., Cui, L., Liu, H., Liang, C., Qiao, Z.** (2017) The Tartary buckwheat genome provides insights into rutin biosynthesis and abiotic stress tolerance. Mol. Plant, 10, 1224–1237. https://doi.org/10.1016/j.molp.2017.08.013

Zhang, X., He, Y., Li, L., Liu, H., Hong, G. (2021) Involvement of the R2R3-MYB transcription factor MYB21 and its homologs in regulating flavonol accumulation in *Arabidopsis* stamen. J. Exp. Bot, 72, 4319–4332. https://doi.org/10.1093/jxb/erab156

Zhang, Y., Liu, T., Meyer, C.A., Eeckhoute, J., Johnson, D.S., Bernstein, B.E., Nusbaum, C., Myers, R.M., Brown, M., Li, W., Liu, X.S. (2008) Model-based analysis of ChIP-Seq (MACS). Genome Biol, 9, R137. https://doi.org/10.1186/gb-2008-9-9-r137

Zhao, C., Liu, X., Gong, Q., Cao, J., Shen, W., Yin, X., Grierson, D., Zhang, B., Xu, C., Li, X., Chen, K., Sun, C. (2021) Three AP2/ERF family members modulate flavonoid synthesis by regulating type IV chalcone isomerase in citrus. Plant Biotechnol. J, 19, 671–688. https://doi.org/10.1111/pbi.13494

Zhao, H., He, Y., Zhang, K., Li, S., Chen, Y., He, M., He, F., Gao, B., Yang, D., Fan, Y., Zhu, X., Yan, M., Giglioli-Guivarc'h, N., Hano, C., Fernie, A.R., Georgiev, M.I., Janovská, D., Meglič, V., Zhou, M. (2023) Rewiring of the seed metabolome during Tartary buckwheat domestication. Plant Biotechnol. J, 21, 150–164. https://doi.org/10.1111/pbi.13932

Zhou, Y., Chen, M., Guo, J., Wang, Y., Min, D., Jiang, Q., Ji, H., Huang, C., Wei, W., Xu, H., Chen, X., Li, L., Xu, Z., Cheng, X., Wang, Chunxiao, Wang, Chengshe, Ma, Y. (2020) Overexpression of soybean *DREB1* enhances drought stress tolerance of transgenic wheat in the field. J. Exp. Bot, 71, 1842–1857. https://doi.org/10.1093/jxb/erz569

Zhou, M., Sun, Z., Ding, M., Logacheva, M.D., Kreft, I., Wang, D., Yan, M., Shao, J., Tang, Y., Wu, Y., Zhu, X. (2017) FtSAD2 and FtJAZ1 regulate activity of the FtMYB11 transcription repressor of the phenylpropanoid pathway in Fagopyrum tataricum. New Phytol. 216, 814–828. https://doi.org/10.1111/nph.14692**Zhu, J.K.** (2016) Abiotic stress signaling and responses in plants. Cell, 167, 313–324. https://doi.org/10.1016/j.cell.2016.08.029

Zhu, Y., Zhu, X., Wen, Y., Wang, Lanhua, Wang, Y., Liao, C., Zhao, M., Li, T., Liu, D., Li, B., Zhu, T., Wang, Lianzhe. (2024) Plant hairy roots: Induction, applications, limitations and prospects. Ind. Crops Prod. 219, 119104. https://doi.org/10.1016/j.indcrop.2024.119104

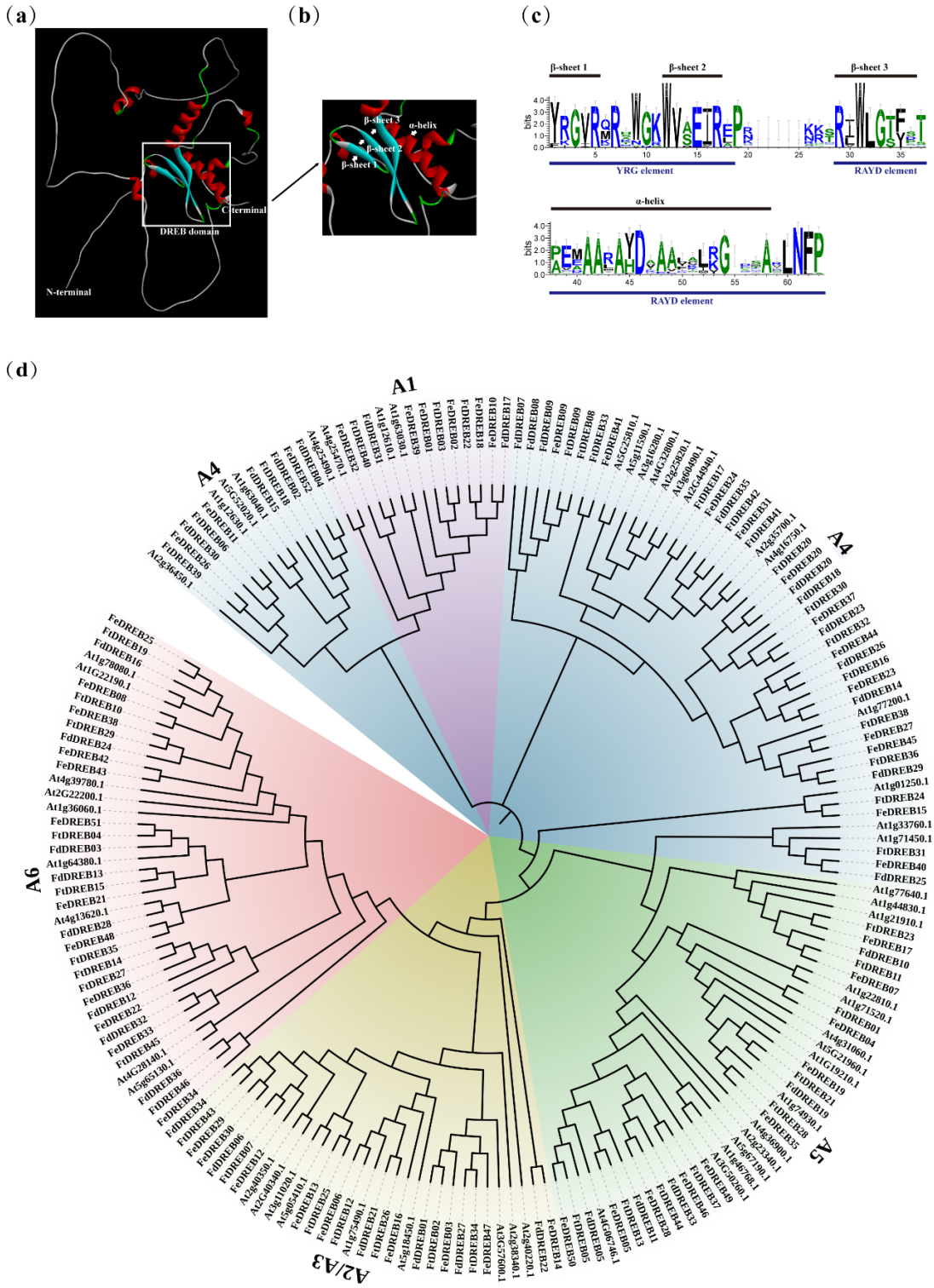

Figure 1 Identification of the DREB family in *F. dibotrys*, *F. tataricum*, *F. esculentum,* and *A. thaliana.*

(a) 3-D structural model of the DREB family from the AlphaFold protein structure database. (b) A magnified view of the 3-D structure of the conserved domain of DREB. (c) Domain sequence logo of the FtDREBs protein was generated by WebLogo. The height of each symbol within the stack represents the relative frequency of the corresponding amino acid at a given position. The β-sheet and α-helix structural elements are positioned above their respective amino acid sequences. Conserved elements are clearly marked. (d) Phylogenetic tree of DREB proteins in *F. dibotrys*, *F. tataricum*, *F. esculentum,* and *A. thaliana*.

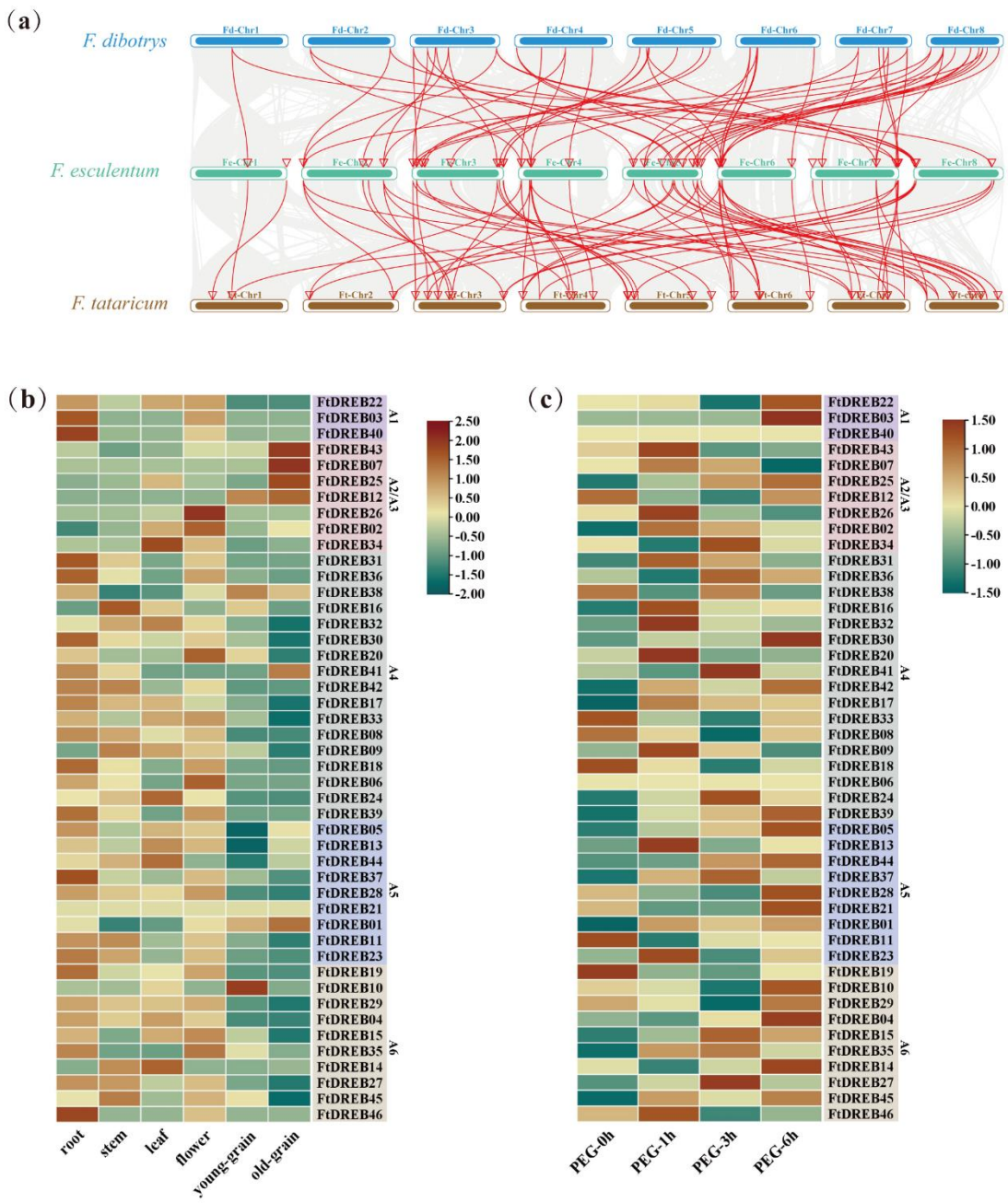

Figure 2 Comparative synteny and expression profiles of *DREBs in Fagopyrum dibotrys, F. tataricum, and F. esculentum.*

(a) Syntenic relationships of *DREB* genes across the three species. Gray lines indicate collinear genomic regions conserved among all three species, while red lines highlight syntenic *DREB* gene pairs. (b) Tissue-specific expression patterns and (c) expression dynamics under PEG-induced drought stress of *DREB* genes in *F. tataricum*. The gradient color scale from olive green (Hex: #006666) to saddle brown (Hex: #993300) indicates the continuum of gene expression levels, with light green representing low expression (normalized log2FC ≤ -1) and dark brown denoting high expression (normalized log2FC ≥ 1). Vertically arranged gene labels are color-coded by phylogenetic clade: Lavender (#77509d): Group A1, Salmon pink (# b76b7f): Groups A2/A3, Sage green (# 708f8c): Group A4, Sky blue (# 366eb6): Group A5, Goldenrod (# a89675): Group A6.

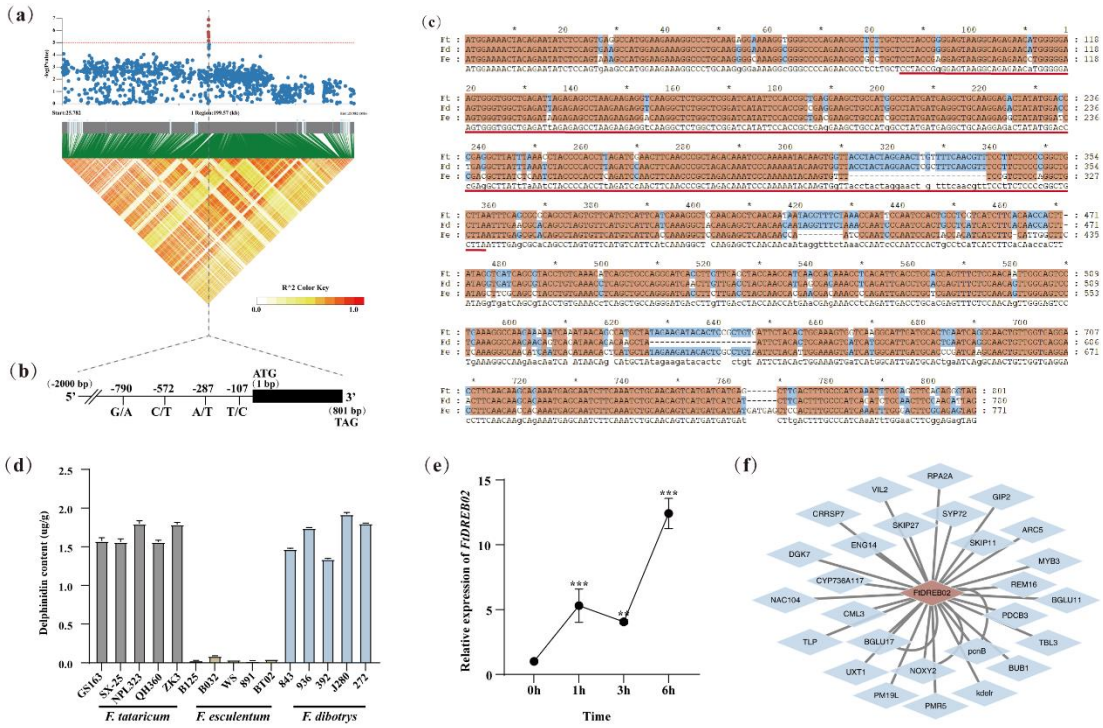

Figure 3 Identification and Functional Characterization of *FtDREB2*.

(a) Local Manhattan plot of the drought-associated GWAS peak containing *FtDREB2*. (b) Genomic architecture of *FtDREB2*, showing SNP distribution and gene structure. (c) Multiple sequence alignment of *FtDREB2* homologs in Tartary buckwheat (Ft), common buckwheat (Fe) and golden buckwheat (Fd), with red underlines highlighting the conserved AP2/ERF domain. (d) Delphinidin content variation among representative accessions of the three buckwheat species. (e) Expression profiles of *FtDREB2* in Tartary buckwheat under 20% PEG-6000-induced osmotic stress. (f) The co-expression network of the top 50 genes identified through WGCNA analysis of PEG-responsive transcriptomes. Quantitative data are expressed as mean ± SD from triplicate biological experiments (n = 3), with statistical significance indicated by asterisks (*P < 0.05, **P < 0.01, ***P < 0.001).

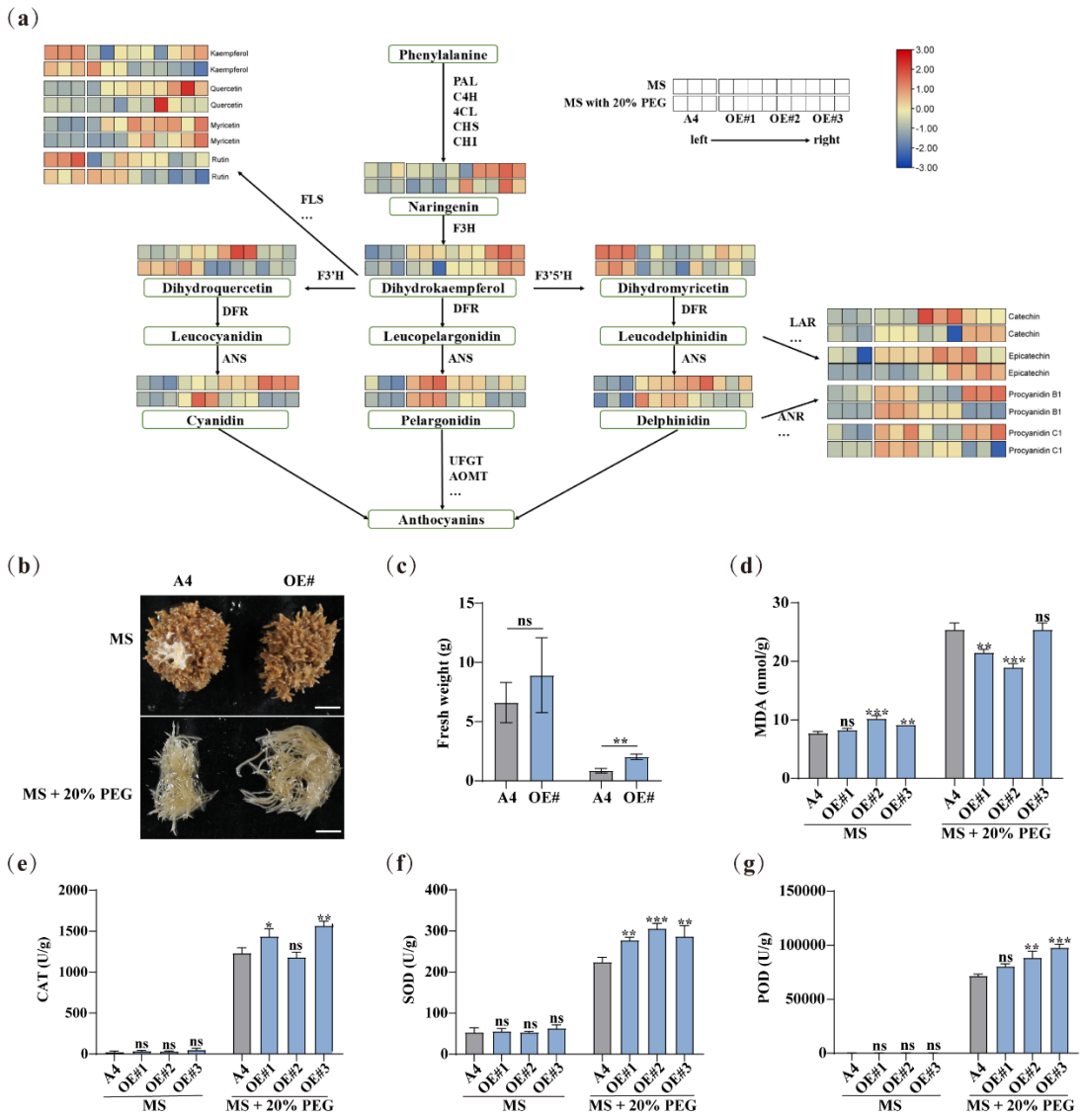

Figure 4 *FtDREB02* overexpression in hairy roots of *F. tataricum*.

Metabolite changes (a) and The phenotype (b) of A4 (Agrobacterium rhizogenes A4 without any plasmid) control lines and *FtDREB02* overexpression lines (OE lines) of Tartary buckwheat hair root under Murashige and Skoog Medium (MS) medium without or within 20% Polyethylene glycol 6000 (PEG 6000) treatment for 30 days. White bars represent 1 cm. (c) Fresh weight of hairy root treated as described in (b). Malondialdehyde (MDA) (d), catalase (CAT) (e), superoxide dismutase (SOD) (f), peroxidase (POD) (g) content of hair root under different culture conditions. Quantitative data are expressed as mean ± SD from triplicate biological experiments (n = 3), with statistical significance indicated by asterisks (*P < 0.05, **P < 0.01, ***P < 0.001).

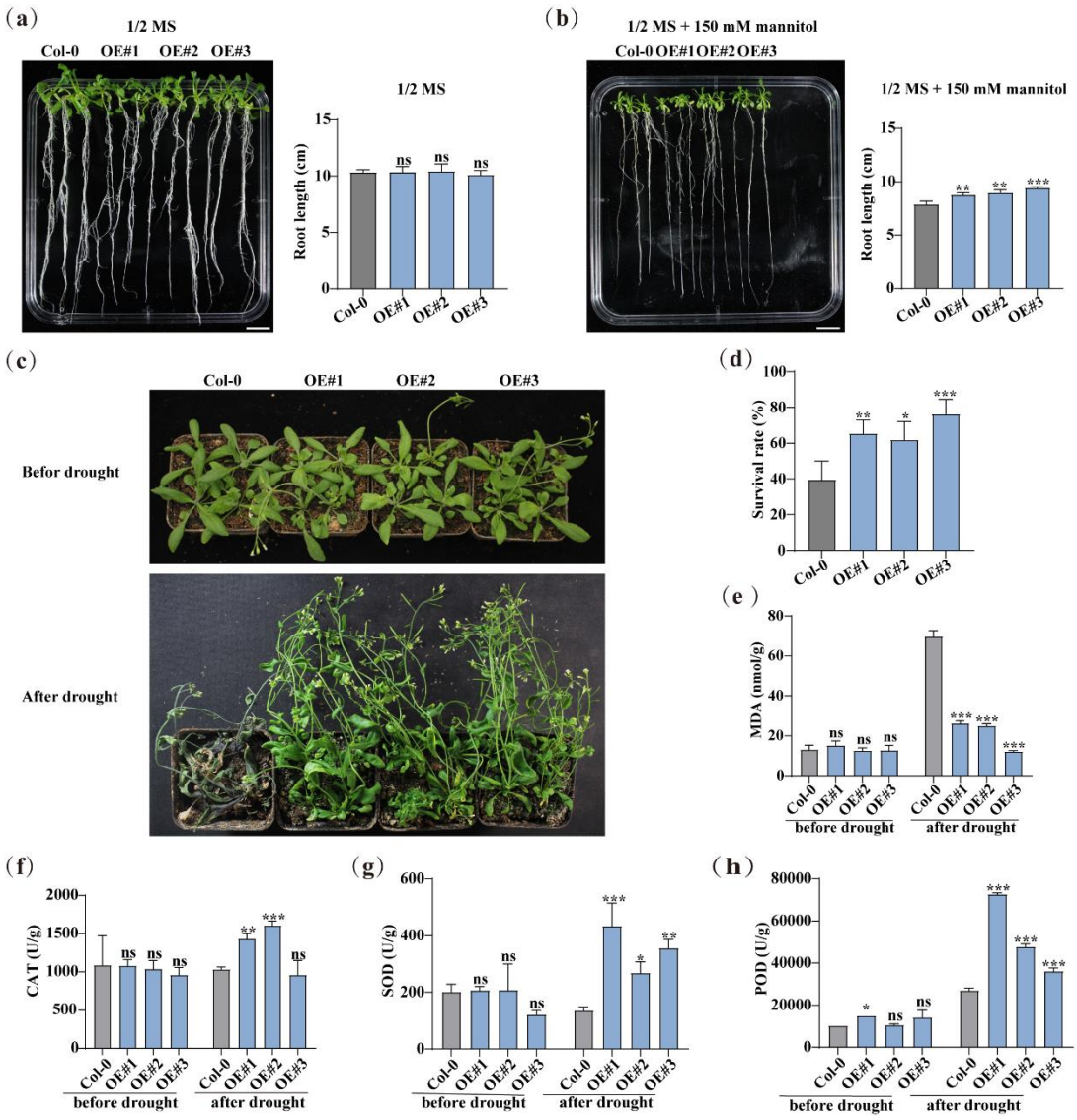

Figure 5 *FtDREB02* Overexpression in *Arabidopsis*.

The primary root length of Col-0 and *FtDREB02*-OE lines grown on MS dishes without (a) and within (b) 150 mM mannitol. White bar represents 1 cm. (c) Arabidopsis plant of Col-0 and *FtDREB02*-OE lines before and after natural drought stress. (d) Survival rate of Col-0 and *FtDREB02*-OE lines treated as described in (c). Malondialdehyde (MDA) (e), catalase (CAT) (f), superoxide dismutase (SOD) (g), peroxidase (POD) (h) content in Col-0 and *FtDREB02*-OE lines treated as described in (c). Quantitative data are expressed as mean ± SD from triplicate biological experiments (n = 3), with statistical significance indicated by asterisks (*P < 0.05, **P < 0.01, ***P < 0.001).

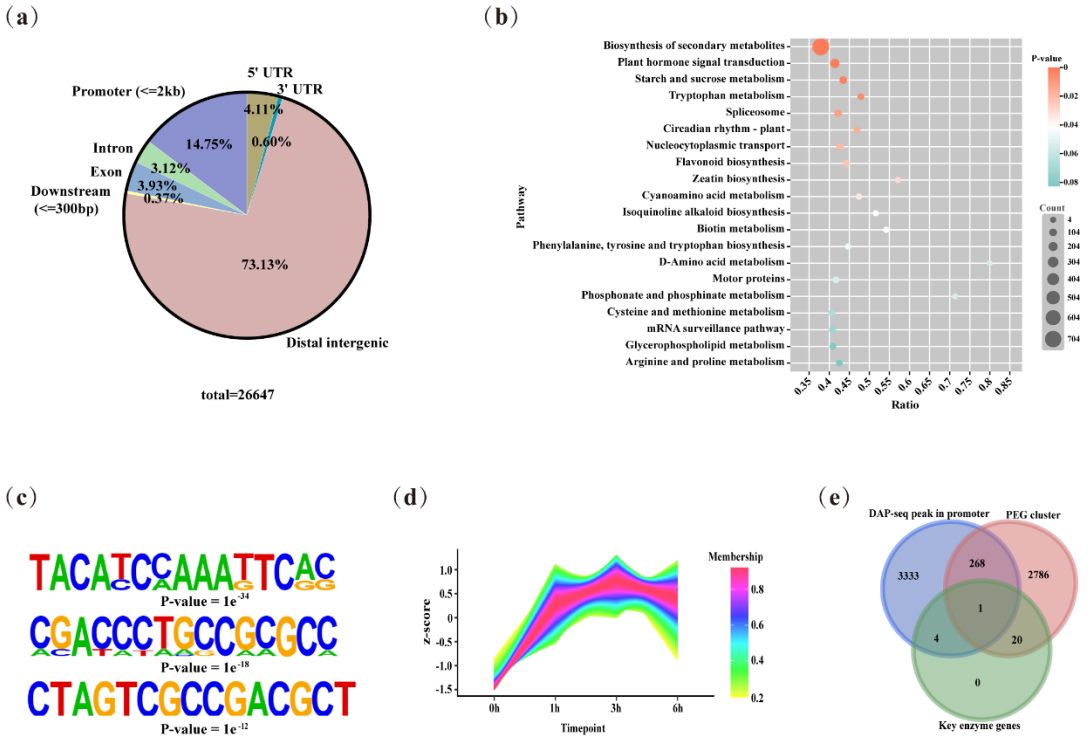

Figure 6 Identification of the *FtDREB02* target genes by DAP-seq and PEG transcriptome.

(a) Distribution of DAP-seq binding sites on the *F. tataricum* genome. (b) The top 20 pathways in KEGG enrichment analysis of genes with DAP-seq binding peaks located within 2kb of the promoter. (c) Conservative motif enriched from recognition interval of *FtDREB02* (partial display). (d) Cluster analysis of gene expression patterns of *FtDREB02* and *FtANS* in *F. tataricum* in the PEG transcriptome. (e) Venn diagram based on downstream gene screening criteria.

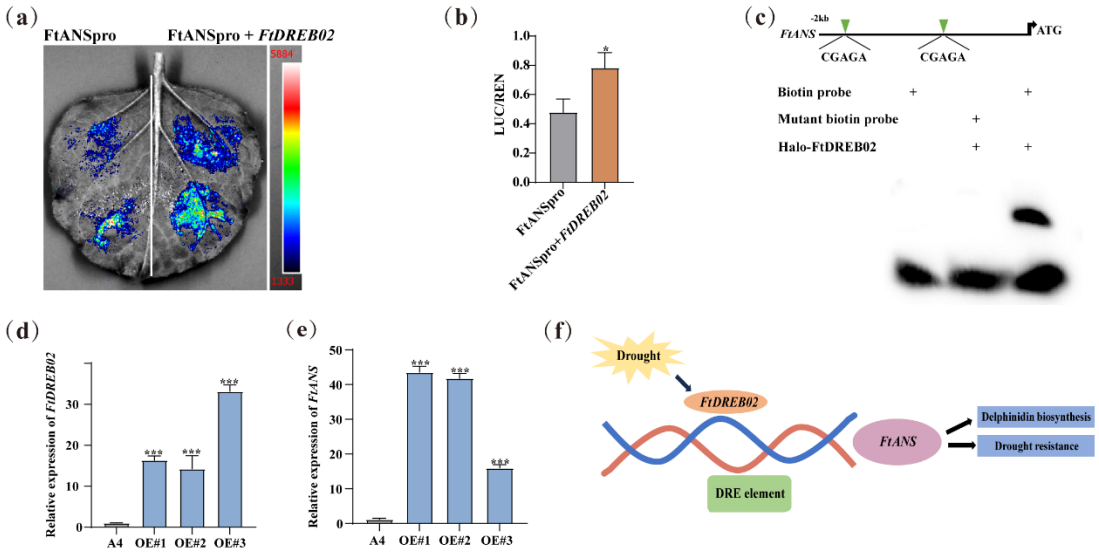

Figure 7 *FtANS* is regulated by *FtDREB02*.

(a-b) Measurement of firefly luciferase (LUC) and renilla luciferase (REN) activities.

(c) EMSA shows *FtDREB02* directly binds to the DRE element of *FtANS* promoter.

(d-e) Relative expression of *FtDREB02* and *FtANS* in *FtDREB02* transgenic hairy roots.

(f) Model diagram for *FtDREB02* under drought stress. In response to drought stress, *FtDREB02* attaches to the DRE element of the *FtANS* promoter, regulating gene expression by activating downstream gene promoter, increasing delphinidin content, and thus enhancing drought resistance. Quantitative data are expressed as mean ± SD from triplicate biological experiments (n = 3), with statistical significance indicated by asterisks (*P < 0.05, **P < 0.01, ***P < 0.001).